CHALMERS
UNIVERSITY OF TECHNOLOGY

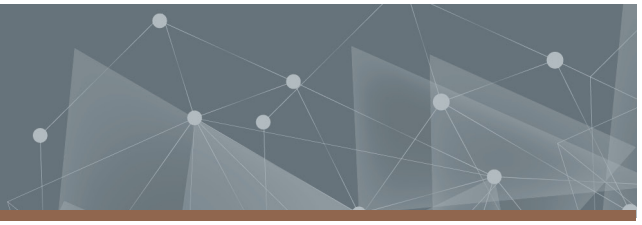

Artificial Infiltration in Rock and Soil

A Comparison of Responses in Central Gothenburg using Numerical Models

Master's thesis in Infrastructure and Environmental Engineering

Hedda Hagman
Albin Nimheim

DEPARTMENT OF ARCHITECTURE AND CIVIL ENGINEERING

CHALMERS UNIVERSITY OF TECHNOLOGY
Gothenburg, Sweden 2021
www.chalmers.se

Master's thesis ACEX30

Artificial Infiltration in Rock and Soil

A Comparison of Responses in Central Gothenburg using Numerical Models

HEDDA HAGMAN
ALBIN NIMHEIM

CHALMERS
UNIVERSITY OF TECHNOLOGY

Department of Architecture and Civil Engineering
Division of Geology and Geotechnics
Chalmers University of Technology
Gothenburg, Sweden 2021

Artificial Infiltration in Rock and Soil
A Comparison of Responses in Central Gothenburg using Numerical Models
HEDDA HAGMAN, ALBIN NIMHEIM

Supervisors: Jenny Palmenäs & Johan Thörn, Bergab
Ezra Haaf, Department of Architecture and Civil Engineering

Examiner: Professor Lars Rosén, Department of Architecture and Civil Engineering

Master's Thesis 2021
Department of Architecture and Civil Engineering
Division of Geology and Geotechnics
Chalmers University of Technology
SE-412 96 Gothenburg
Telephone +46 31 772 1000

Department of Arcitecture and Civil Engineering.
Gothenburg, Sweden 2021

Artificial Infiltration in Rock and Soil
A Comparison of Responses in Central Gothenburg using Numerical Models
Hedda Hagman
Albin Nimheim
Department of Architecture and Civil Engineering
Chalmers University of Technology

Abstract

Underground constructions can cause lowering of the groundwater table, due to groundwater leakage into the structure. To minimize the risk of drawdown, artificial infiltration can be implemented which can maintain or raise the groundwater table to a desired level. Water can be infiltrated either in rock or soil, and observation data has shown that the two materials exhibit different responses. In literature, limited amount of research has been conducted comparing the responses between rock and soil infiltrations and it was therefore of interest to investigate this further.

This thesis aimed to compare the responses obtained from rock and soil infiltration using numerical finite difference modelling. To enable a systematic comparison between the different approaches two types of models were created, using Excel and GMS MODFLOW. Consequently the thesis also resulted in a comparison between the models, to conclude which model approach could simulate the observed data but also to see how the characteristics of the models affected the results. In addition, a risk object, which in this case is a building sensitive to groundwater fluctuations, was included to exemplify the results obtained from the models by suggesting the most suitable infiltration approach. The comparison was applied to a stretch of the Västlänken project, which is a railway tunnel currently being constructed in Gothenburg, Sweden.

The results from both models show that the response generated from rock infiltration have more of a linear response, compared to soil infiltration which demonstrated an exponential trend. The results from the Excel model were correlated to the observed data when it comes to the propagation of the responses, indicating a more diffusive response in rock compared to soil. The GMS MODFLOW model however, did not show this type of pattern. Both numerical models managed to simulate the differences in responses, but to which extent the results coincide with the observed data varied. For the risk object, it was suggested that rock infiltration might be the best option since a more linear response makes it easier to predict how much the levels will be raised. Further, the exponential response from a soil infiltration would require the infiltration facility to be located close by, which might be difficult since the area is densely built.

Keywords: Artificial infiltration, Underground constructions, Numerical modelling, Spreadsheet application, GMS MODFLOW, drawdown.

Acknowledgements

We would like to take the opportunity to thank our supervisors from Bergab, Jenny Palmenäs and Johan Thörn, for guiding us through the process of creating this Thesis. We would also like to thank them for taking the time to meet with us every week and supporting us through this journey. Additionally, we would also like to give thanks to Bergab and the people there who have helped us with field work, modelling and provided us with information regarding Västlänken.

Further, we would also like to thank Ezra Haaf who has been our supervisor at Chalmers and assisted us with the process of the thesis. At last, we would also like to thank our examiner, Lars Rosén, and our opponents, Veronica Falk and Micheal Odhiambo, for your useful input in this project.

Hedda Hagman and Albin Nimheim, Gothenburg, June 2021

Contents

List of Figures

List of Tables

1
Introduction

When constructions underground are built the natural groundwater flows are altered and leakage into the construction will occur (Axelsson & Follin, 2000). This water which flows into the constructions below the groundwater table, can result in subsidence due to groundwater drawdown (Yoo, 2016). This subsidence can damage buildings, municipal piping, or surrounding vegetation for example. To minimize the damage caused by the lowering of the groundwater table, artificial infiltration can be used to counteract the drawdown (Fetter, 2014). Artificial infiltration can be defined as non-natural infiltration of water into an aquifer which results in a raise of the groundwater table.

In recent years, artificial infiltration has been implemented in several underground constructions in Sweden, and one example is the Västlänken tunnel which is currently being constructed in Gothenburg (Vestin et al., 2016). Further, the tunnel will be constructed in both rock and soil, as can be seen in the figure 1.1, and will be built beneath areas in the city were buildings with sensitive foundations are located.

The Swedish Transport Administration [Swedish: Trafikverket] has gathered groundwater data since 2012 to monitor the groundwater levels before and during the construction of Västlänken (Trafikverket, 2019). This data is gathered to understand how the groundwater levels naturally fluctuate but also how the construction will impact the groundwater table in the city. Consequently, this information is used to establish action levels, which states how much the groundwater surface can fluctuate before possible damage can be expected (Vestin et al., 2016). The action levels are connected to risk objects, which can be for example a certain building with a foundation sensitive to groundwater fluctuations. The Swedish Transport Administration has decided to use artificial infiltration in addition to grouting and sealing, to maintain the groundwater levels impacted by the Västlänken tunnel.

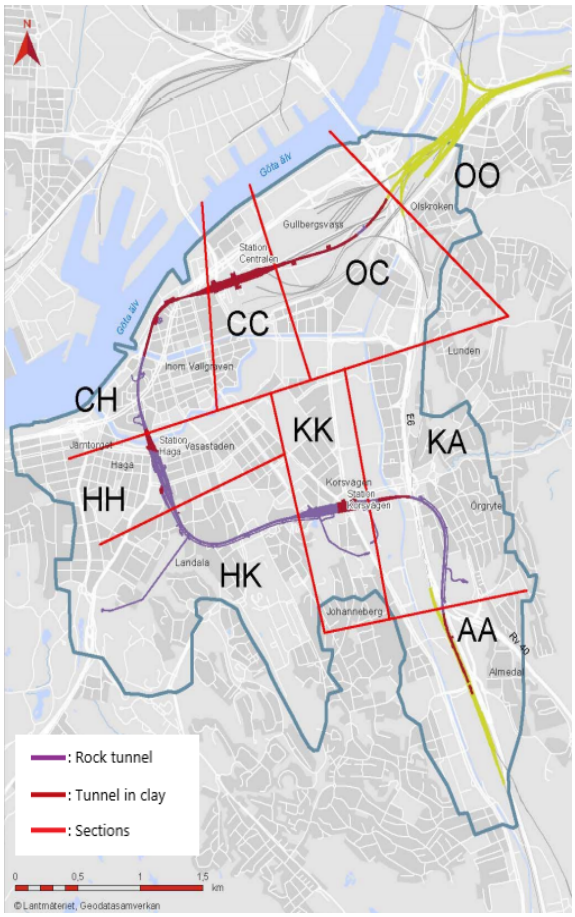

Figure 1.1: Map of Västlänken in Gothenburg, with abbreviations of the different stretches of the project. Modified from Trafikverket (2016c).

Artificial infiltration is applicable for both shallow and deep aquifers (Zhang et al., 2017). Depending on the subsurface characteristics at the site, water can be infiltrated at different elevations e.g. at ground level or from the underground construction, and in different types of materials such as soil and rock (Lindström & Kveen, 2005). The approaches for infiltrating water in these materials differ, infiltration into the soil layer is usually done from the ground level where water is directly infiltrated into the aquifer using a well (Vägverket, 2000). In rock however, water can be infiltrated from inside the construction into the rock through a borehole, which reaches the aquifer through the fractures in the rock (Olofsson & Palmgren, 1994). Further, when infiltrating water in urban areas, such as Gothenburg, it is important to take into account both the groundwater lowering that infiltration aims to mitigate, but also the risk of local peaks near the infiltration point (Vestin et al., 2016). This must be carefully considered since exceeding the lower level can result in subsidence, and on the other hand exceeding the upper level can cause damages such as flooded basements.

Since the Västlänken tunnel is constructed in both rock and soil it makes it possible to infiltrate water by using previously described approaches. When looking at observed data from infiltration tests preformed in rock and soil, the responses from the infiltrations vary, seen in figure A.1. As the tunnel stretch includes risk objects and strict action levels, it is appropriate to know which type of responses are generated from rock and soil infiltrations, as the properties and preconditions differ between them.

Previous studies have been performed examining different aspects of artificial infiltration in relation to underground constructions (Phien-wej et al., 1998; Yoo, 2016; Zhang et al., 2017; Zheng et al., 2019). However, only a few studies such as Olofsson and Palmgren (1994) and Vägverket (2000) mention the differences between rock and soil infiltrations but do not perform a systematic comparison of the obtained responses. Due to the lack of literature comparing artificial infiltration in rock and soil, it is of interest to investigate how the responses vary between these materials. In this thesis, four infiltration sites will be analyzed; two infiltration tests in soil and two permanent infiltrations in rock. The comparison will be performed by creating two numerical models, which are solved using the finite difference method. The first model has a simpler approach using a spread sheet created in Excel and the second is created in GMS, which runs MODFLOW to solve the groundwater flow equation. It was of interest to see how well the results correlate to the observed data, and to see if both models are capable of distinguishing the responses in rock and soil infiltrations. To give the comparison a context, the study will also investigate the most suitable approach for a case area in Gothenburg with a risk object, which is a building with timber foundation sensitive to groundwater fluctuations.

1.1 Aim and Research questions

The thesis aims to investigate and systematically compare the responses obtained from rock and soil infiltrations by utilizing observed groundwater data and two different numerical modelling approaches. Two type of models are used to enable a comparison of the results, different approaches and to be able to verify obtained responses in rock and soil. The primary location of interest for this study is the stretch from Centralen to Haga in the Västlänken project, where both infiltrations in soil and rock have been executed. The area can be seen in figure 1.1, and is referred to as CH in the map. In the area, a block called *Residenset* is located, which includes a risk object with a sensitive foundation for changes in groundwater levels. Hence, a reasoning about the most suitable approach for maintaining a constant groundwater level, will be conducted based on the obtained model results.

1. What distinguishes the groundwater response between rock infiltration and soil infiltration?
2. How do the results from GMS MODFLOW and Excel differ between each other?
3. Based on these findings, which infiltration method is the most suitable for infiltrating water at Residenset?

1.2 Scope

In this study only the area around Residenset will be of interest, which limits the type of hydrogeology and geology investigated in the models. In the area a hydrogeological conceptualization has already been performed. Consequently this thesis will not focus on developing site characteristics for the mentioned area, but instead add to the already developed conceptualization.

The models constructed are simulated as steady-state, thus not taking into account any temporal disturbances in the area. Examples are the Västlänken tunnel which is currently being built and the leakage into the Göta tunnel. Additionally, the models are simplified and constrained to the data available for the infiltration facilities.

1.3 Methodology - Research questions

The method of how the three research questions listed in section 1.1 will be answered, can be seen in figure 1.2. As mentioned previously, the study will focus on constructing two different numerical models with varying complexity, which will be based on literature findings, study area, observed data and calculated hydrogeological parameters. The results from the models will be used to answer the three research questions. Research question (1) covers the comparison of rock and soil responses, and will be answered using graphs of the response curves from the infiltrations. Next, the differences between the two models, Research question (2), will be evaluated based on how reliable the models are in comparison to the observed data. Finally, the findings from questions (1) and (2) will be used together with the site description presented in chapter 3, to discuss research question (3) which includes a suggestion of the most suitable infiltration method for the risk object at Residenset.

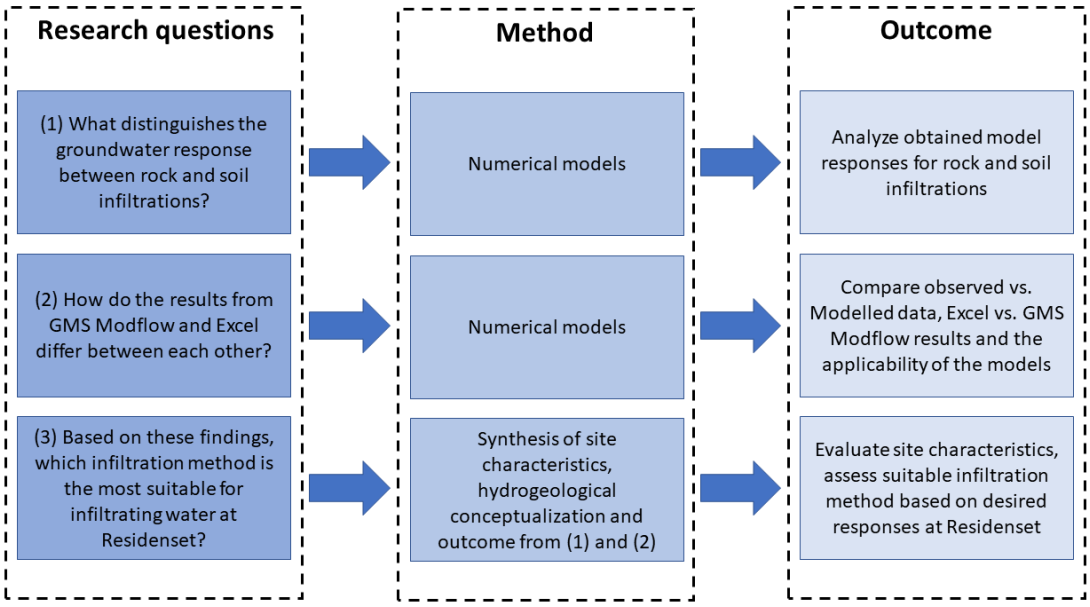

Figure 1.2: Flowchart displaying how the research questions will be answered.

2
Artificial infiltration

As mentioned in chapter 1, underground constructions can cause non-natural fluctuations in the groundwater table. To minimize and control groundwater drawdown due to constructions, artificial infiltration can be implemented in the area that is influenced by the construction (Cashman et al., 2020). Artificial infiltration is a technique where the ground water level is raised by either induced percolation from the ground surface or when water is directly infiltrated in the aquifer through either a well or borehole. This chapter will cover the specifics and differences of two separate techniques, artificial infiltration into crystalline rock through boreholes drilled in the inner surface of an underground construction, and artificial infiltration into soil from a well constructed at ground level. These types of infiltrations will be referred to as rock infiltration respectively soil infiltration in this study.

2.1 Groundwater in rock and soil

Groundwater generally flows from high situated areas to low lying areas according to Darcy's law (Fetter, 2014). Flow paths within the ground vary depending on the characteristics of the material. In a porous media groundwater flows in voids, contrary to crystalline rock, where water flows in fractures. Regarding rock, the permeability is often larger in the shallow rock closest to the soil layer compared to the deeper rock mass (Gustafson, 2009; Kvartsberg et al., 2021).

Aquifers are geological units made of porous media or rock, where water can flow and be extracted in sufficient amounts (Fetter, 2014). Further, the aquifers can vary in characteristics and either be unconfined, leaky or confined. The latter one is sealed by a confining layer with a low permeability. However, in many aquifers the overlying layer is often leaky and water is slowly seeping through the confining layer.

2.2 Infiltration in soil

Artificial infiltration in soil is here defined as a pipe well which has been drilled from ground level down into an aquifer located in soil (Olofsson & Palmgren, 1994). According to Olofsson and Palmgren (1994), water flows horizontally from the well into the soil and the infiltration flow is regulated by the properties of the soil. Furthermore, to determine the infiltration flow and the most optimal location for a well, information about the geological and hydrogeological characteristics in the area need to be studied. An advantage with this type of soil infiltration is that the well can precisely infiltrate water into an aquifer, and avoid layers with poor infiltration capacities (Cashman et al., 2020). An additional advantage according to Olofsson and Palmgren (1994), is that soil infiltration is easier to implement as a quick temporary measure, compared to rock infiltration.

The first step to design an infiltration well is to determine at which depth the well will be situated, which depends on the depth of the water bearing layer (Phien-wej et al., 1998). Secondly, the diameter of the borehole needs to be determined, which is related to the intended infiltration flow. Figure 2.1 shows an example of a well used for soil infiltration. The Well casing has to be robust enough to keep the well open and prevent the borehole from collapsing due to the acting pressure on the pipe (Ahmed et al., 2014; Cashman et al., 2020; Olofsson & Palmgren, 1994). On the outside of the well casing, the well screen is mounted (Cashman et al., 2020). This part of the well is permeable with openings, whereupon the infiltration water is able to flow out from the pipe into the surrounding filter pack. The openings in the well screen have different shapes and sizes, and depends on the coarseness of the surrounding filter pack (Ahmed et al., 2014).

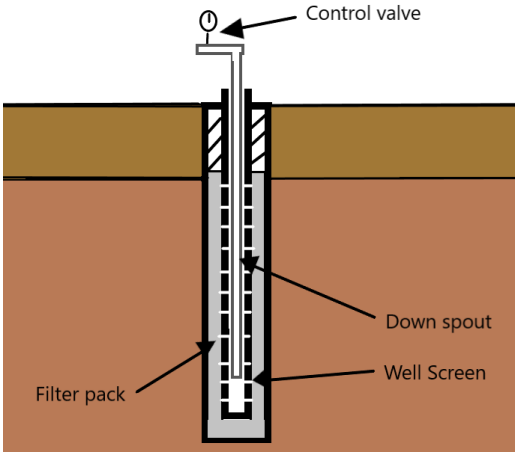

Figure 2.1: An example of a soil infiltration well. Modified from Cashman et al. (2020).

According to Cashman et al. (2020), almost every well is prone to clogging. Clogging can occur due to the direction of the water flow. As water is pumped down into the well, suspended solids, particles, biological growth and air bubbles can be transported with the flow to the lower part of the well. Further, these clogging agents may get stuck either on the inside or the outside of the well and block openings and voids, thus restricting paths water can flow through. Hence, clogging leads to a reduction in infiltration efficiency and can be anticipated for all infiltration wells in soil. Another existing problem regarding infiltration wells in soil is piping (Olofsson & Palmgren, 1994). This problem occurs if too high water pressure is applied resulting in water flowing alongside the well casing. However, if the pressure is too low the responses in the surrounding area will decrease and a higher risk of clogging will occur.

2.3 Infiltration in rock

Infiltration in rock can be applied for different reasons such as poor infiltration capacity from soil infiltration or lack of space e.g. in an urban city. Infiltrating water from an underground construction into the bedrock or shallow rock has proven to be a good approach in several projects to both maintain and restore groundwater levels (Olofsson & Palmgren, 1994). In addition, according to Olofsson and Palmgren (1994) this type of method has proven to be particularly successful when the rock is covered with clay and no intermediate friction soil layer exists. Furthermore, the method includes less risk of long-term problems such as clogging compared to soil infiltration, but on the other hand contain more uncertainties in the earlier phases when constructing the infiltration (Olofsson & Palmgren, 1994). These problems at an earlier stage are mostly related to the position of the boreholes, which may have been incorrectly assessed in regard to the heterogeneity of the rock.

The borehole is drilled from the inside of an underground structure, with a borehole length either reaching the shallow rock or the soil layer on top of the rock (Olofsson & Palmgren, 1994). After the borehole has been drilled, a sealing packer is installed in the borehole to prevent the water from flowing back into the construction. The borehole and packer can be seen in figure 2.2.

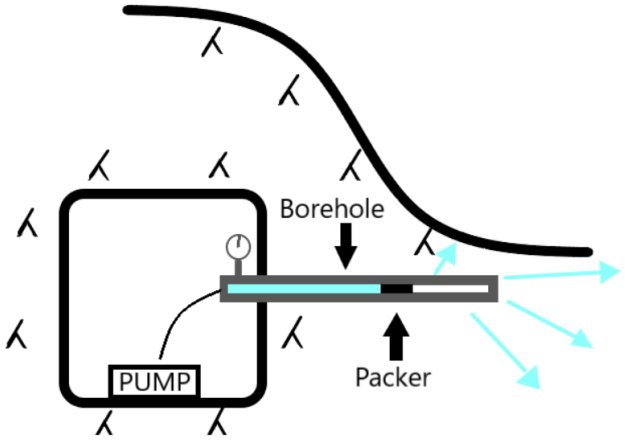

Figure 2.2: Rock infiltration performed inside an underground construction. Modified from Olofsson and Palmgren (1994).

When the borehole is drilled to the shallow rock, it is important to reach a water bearing fracture, so that the water can be transported further to the permeable soil layer (Olofsson & Palmgren, 1994). When water flows through the fractures in the rock it will spread quantities of water over a larger area in the aquifer. Groundwater flows in all fractures but the flow differ in magnitude depending on the resistance in each individual fracture (Gustafson, 2009). Further, the flow resistance is proportional to the aperture of the fracture itself. When infiltrating water through a borehole, the water pressure must always be higher than the current pressure in the aquifer to enable a successful infiltration (Olofsson & Palmgren, 1994). However, if the water pressure is too high this can instead result in that the overlaying soil layers becomes disrupted, which causes a change in permeability. In addition, a too high pressure can also lead to unwanted channels in the overlying soil layer.

3
Study area

This study will focus on the stretch of Västlänkstunneln from station Centralen to Haga, see figure 1.1. The area contains both infiltration facilities in rock and soil, where some of them are today used permanently while others were constructed on a test basis. The stratification in the area has been conducted through sampling and testing, executed in both rock and soil (Trafikverket, 2016b, 2016c). The study includes already existing underground constructions such as Götatunneln. Those constructions affect the groundwater level in the area significantly, where drawdown have been observed in the lower aquifer in connection to the structures (Trafikverket, 2016d). As mentioned earlier, it is important to prevent and restrict groundwater lowering since buildings with sensitive foundations are located in the area. One such example is the building located in the block referred to as Residenset, which will be described later in this chapter.

3.1 Hydrogeological conditions

The hydrogeological conditions in the area vary spatially in both rock and soil. Different investigations have been carried out to establish the general hydrogeological settings, and the construction of Västlänken have been adjusted to adapt to these conditions. Due to the close proximity to Götatunneln, many hydrogeological tests have been performed previous to the commencement of the Västlänken project. This data has then been used together with data gathered for the Västlänken project, to form a conceptual model about the hydrogeological conditions at the site.

3.1.1 Hydrogeological conditions - in soil

The data to establish the hydrogeological conditions in soil for Västlänken have been gathered through probings, well measurements, pore pressure readings, pumping tests and pulse tests (Trafikverket, 2016c). Both sieve analysis and pulse tests have been conducted recently for the Västlänken project. Additionally, infiltration tests and pump tests have been performed due to the construction of Götatunneln close by. Wells in the area are both constructed to measure groundwater levels but also to define the hydrogeological conditions for the site, such as the stratification of the soil layers and their respective hydraulic conductivity.

Investigations have shown that the area generally consists of bedrock covered by friction soil, clay and fill material, in varying thicknesses over the area, see figure 3.1 (Trafikverket, 2016c). The thickness of the friction soil varies between 0.5-3 meters, and increases approaching the Göta älv and Stora Hamnkanalen, which can be seen in figure 3.2. In terms of type of soil material the sieve analysis shows that the friction soil generally consist of relatively well sorted sand. Around the rocky outcrops, seen in figure 3.2, the friction layers are often thinner, closer to 0.5-1 meters, and can also be found at surface level. In the northern part of the area, the clay depths can reach around 100 meters and the thickness of the clay layer is decreasing towards the south, where maximum clay depths around 30 meters are more common. Closest to the surface, a fill material can be found which both varies in thickness and type of material.

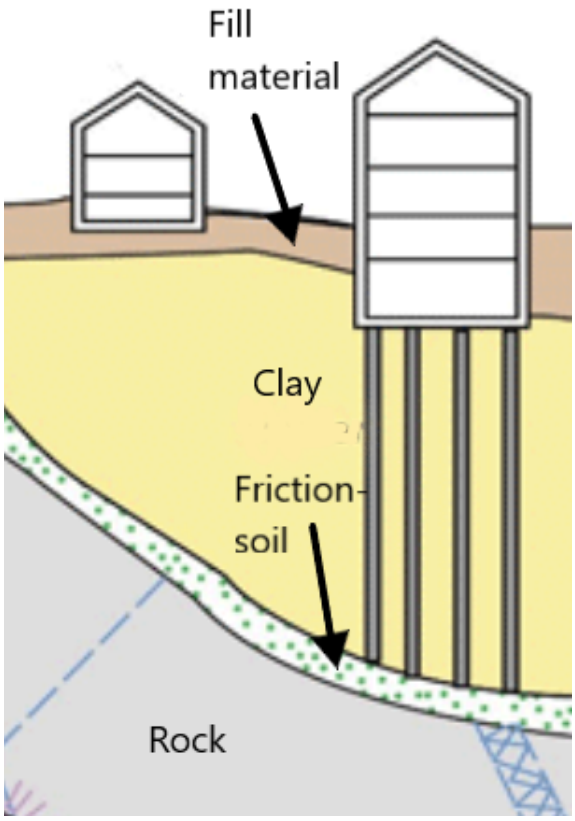

Figure 3.1: General stratification in the area. Modified from Trafikverket (2019)

Figure 3.2: Soil map of the studied area, including Västlänkstunneln in rock and soil and Kämpebron. Modified from Trafikverket (2016c).

Hydraulic parameters have been assessed from the performed pump and infiltration tests at Kämpebron, which can be seen in figure 3.2 (Trafikverket, 2016c). The results from the tests can be found in table 3.1.

Hydrogeological Parameter	Values
Hydraulic Transmissivity, T_{local}	1.5E-0.4 m^2/s
Hydraulic Transmissivity, $T_{regional}$	1.3E-0.5 m^2/s
Influence radius, R_e (flow 6.5 l/min)	150-200 meters

Table 3.1: Hydrogeological parameters from pumping and infiltration tests at Kämpebron.

In the study area a widespread lower confined aquifer in the friction soil has be identified (Trafikverket, 2016c). The upper unconfined aquifer is less connected and can most commonly be found in the overlying fill material. The upper and lower aquifers can be hydraulically connected at the recharge zones, which is where the friction soil or fill material emerge at the surface and where the clay layer is missing (Trafikverket, 2017a, 2017c, 2017e, 2017f). The recharge zones can generally be found close to the rocky outcrops where the friction soil is visible, which can be seen in figure 3.2.

In the studied area two separate rocky outcrops can be found, Kvarnberget in the north and Otterhällan in the south (Trafikverket, 2016b). On the east side of Otterhällan the groundwater flow is generally to the east and the flow is the opposite on the western side (Trafikverket, 2017a, 2017d). The same pattern can be found around Kvarnberget (Trafikverket, 2017e, 2017f). Additionally, the groundwater levels are generally the lowest closet to the river and then increase in the eastern direction. The water levels in the Göta älv varies between -0.2 to +0.4. The upper aquifer is at some locations hydraulically connected to the Göta älv and Stora Hamnkanalen, which can most clearly be seen in the groundwater wells nearby and to the north of Stora Hamnkanalen (Trafikverket, 2017a, 2017e, 2017g, 2017h). The lower aquifer is generally not considered to be in contact with the Göta älv or Stora Hamnkanalen. However, what has been seen is that some wells close to the river follow the same fluctuations in groundwater level as the Göta älv, which indicates that hydraulic contact may be present to some degree.

3.1.2 Hydrogeological conditions - in rock

Sampling and rock mapping have been carried out in the area to investigate the properties of the rocks (Trafikverket, 2016a). Based on the results from the investigation, it was determined that both Kvarnberget and Otterhällan are gneiss with a distinct foliation, but with differences in rock composition (Trafikverket, 2016a). In the area an interpretation of fractures zones has been conducted in the Västlänken project, based on a bedrock model created on behalf of The Swedish Transport Administration (Trafikverket, 2016b). Figure 3.3 shows a map outlining fracture zones in the area and it can be seen that the area consists of two different types of fractures, steep fractures and fractures with a dip towards west. Further, at Otterhällan the fractures in north-south (N-S) and east-west (E-W) directions have been determined to be water bearing (Trafikverket, 2016b). According to Trafikverket (2016a) the fracture set striking in E-W direction, located in the northern part of Otterhällan are regarded as highly permeable due to erosion. Furthermore, the rock is also heavily foliated with one of the main fracture sets being parallel to the foliation and several steep and open fractures can be found at Otterhällegatan striking in E-W direction.

To determine the rock conductivity at Otterhällan, water loss tests on existing boreholes have been conducted (Trafikverket, 2016b). These tests were performed in three different segments for each borehole and resulted in rock conductivities approximately between 1E-08 to 2E-07 (Trafikverket, 2016b). As mentioned in 2.1, the hydraulic conductivity can be anticipated to be higher in the shallow rock (Kvartsberg et al., 2021). This is based on that shallow rock tends to contain more fractures, thus generating a higher conductivity. In addition, the hydraulic conductivity alternate more frequently in shallow rock compared to uniform rock masses.

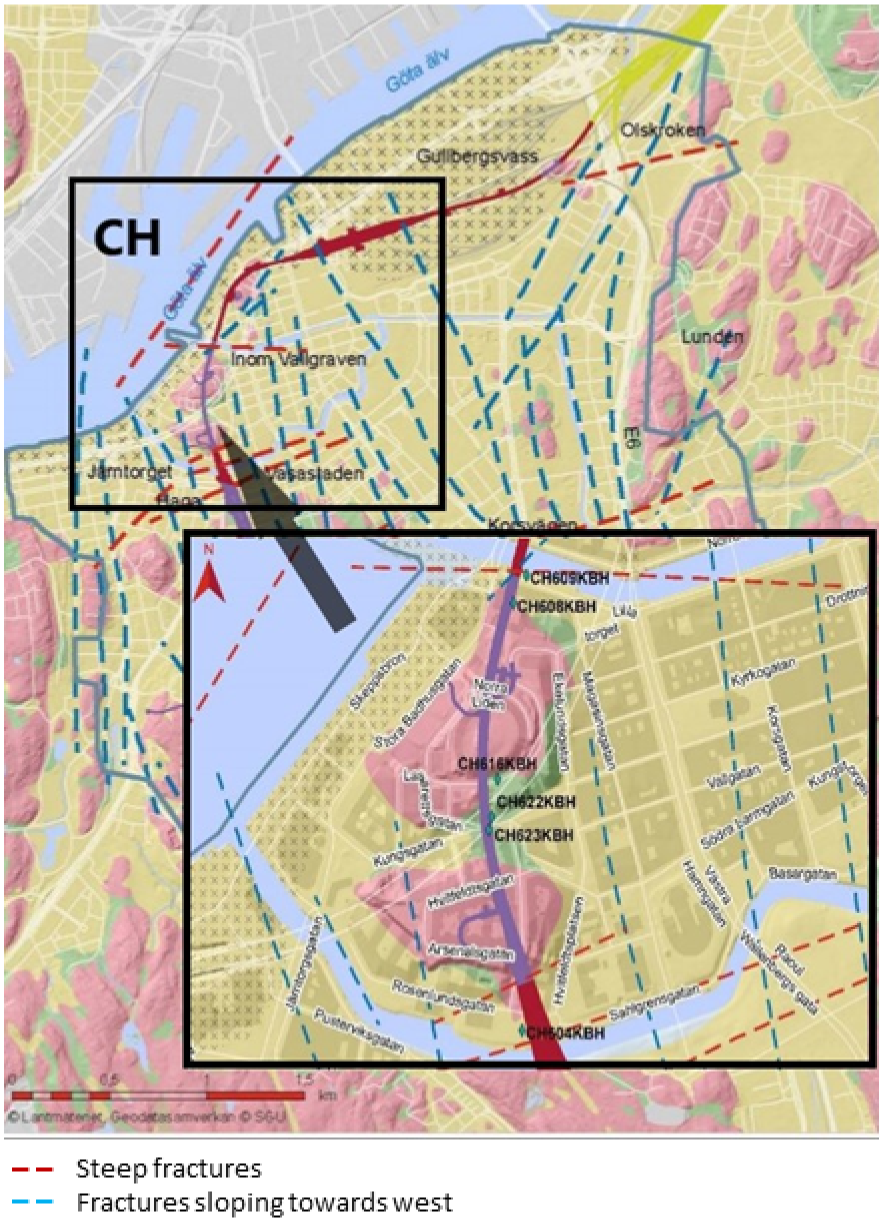

Figure 3.3: Fracture map for Gothenburg and the studied area. Modified from Trafikverket (2016b).

3.2 Case Study - Residenset

Within the study area, a smaller block called "Inom Vallgraven 53" can be located. The block can be seen in figure 3.4, and will be referred to as Residenset in this study. Within the block, the county administrative board of Västra Götaland resides. Västlänkstunneln will be constructed beneath the block and Götatunneln is situated to the east, which can be seen in figure 3.4 as a black shade and blue lines respectively. In the area, Otterhällan can be found to the south, with emerging friction soil close to the surface (Trafikverket, 2017b). Hence, recharge zones can be located in the area, possibly hydraulically connecting the lower and upper aquifer. In general, Residenset follows the same stratification as the larger study area, with bedrock and shallow rock, followed by friction soil, clay and fill material closest to the surface. In the fill material a local upper aquifer can be found and in the friction soil a confined lower aquifer has been identified.

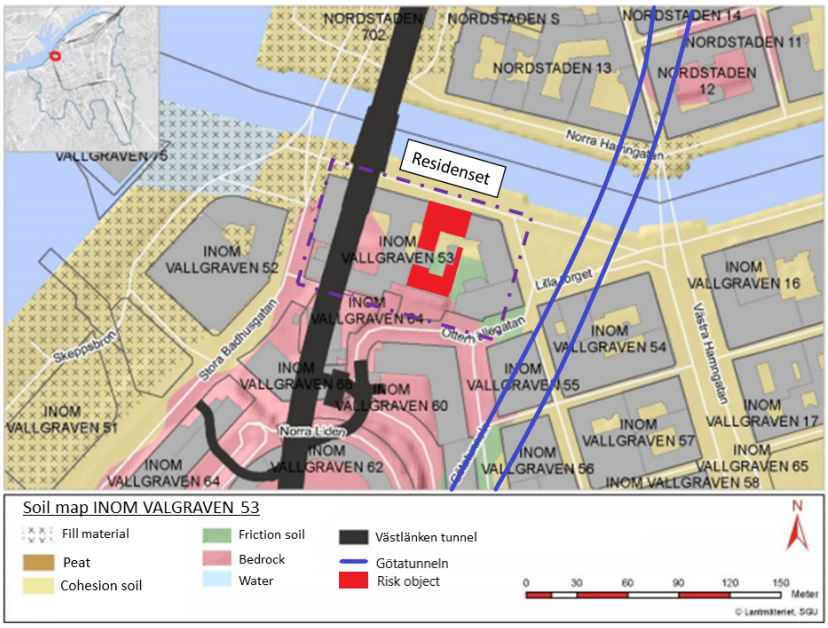

Figure 3.4: The area of Residenset.

Within the area of Residenset the building marked in red, see figure 3.4, is considered as sensitive for groundwater fluctuations in both upper and lower aquifers (Trafikverket, 2017b). This is due to its foundation is partly built with timber. When the groundwater in the aquifer is lowered the timber is exposed to oxygen which results in that the material can be decomposed, and the building can subside. The other buildings in the neighbourhood is built upon the bedrock and therefore not defined as sensitive to groundwater fluctuations.

Due to the sensitive foundation of the building, action levels have been defined for high and low groundwater levels. The lower action levels for the underlying confined aquifer are due to preventing subsidence of the overlying clay layer. Further, the low action levels for the upper unconfined aquifer exists to prevent the wooden foundation from being exposed to oxygen. Table 3.2 shows the low action levels for the upper and lower aquifers in the groundwater wells connected to the risk object. The table also shows high action levels, for the upper aquifer. This is of concern since when infiltrating water in the lower aquifer, the pressures increase and may cause flooded basements in the area if the upper and lower aquifer are connected.

Well	Aquifer	Action level - Low 1	Action level - Low 2	Action level - High
GW1916A	Lower	+0.94	+0.64	-
CH4817O	Upper	+0.89	+0.66	+1.72

Table 3.2: Action levels for Residenset. "Action level - Low 1" refers to when the cause of the drawdown should be investigated, while "Action level - Low 2" refers to a critical groundwater level where measures must be taken immediately. The reference system RH 2000 is used.

4

Method

The method and workflow is schematically described in figure 4.1. The general conceptualization was based on chapter 3 and describes the assumptions made in the area to construct the models. Subsequently, the observed data was gathered for the rock and soil infiltration sites that will be investigated in this study. This was thereafter used to analytically calculate the hydrogeological parameters needed for the models. When all data was gathered and the parameters were calculated, the models were created. Model calibration was performed based on observed data. Lastly, the results were processed into change in head plots, response curves and modelled data tables.

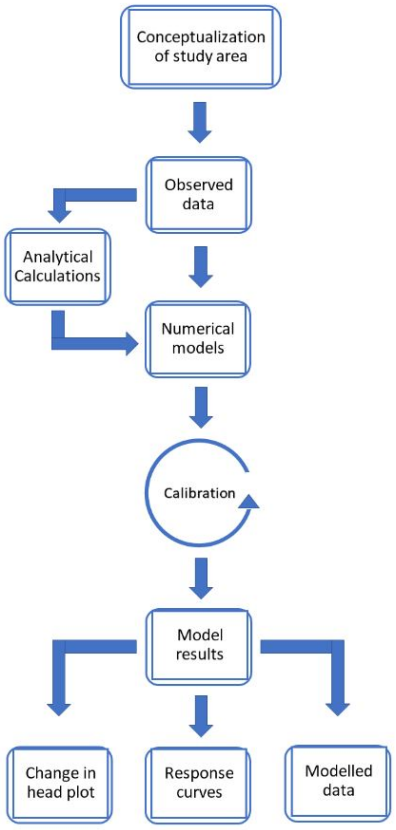

Figure 4.1: The Work flow of this thesis illustrated in a basic flowchart.

4.1 General conceptualization of the area

The boundary conditions chosen for the area are based on the conceptualization presented in chapter 3. As mentioned, the stratification have been generalized to include fill material, clay, friction soil, shallow rock and bedrock, which can be seen in figure 4.2. Further, the dominating direction of fractures at Otterhällan have been interpreted to be E-W direction. Additionally, as stated in chapter 3, these fractures are considered to be water bearing, which was an assumption for the fractures simulated in this study.

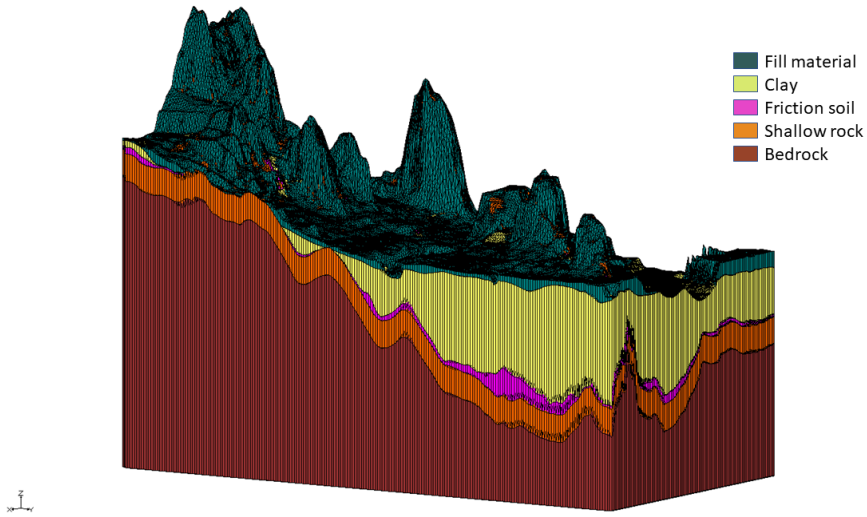

Figure 4.2: Conceptualization of the stratification with the five layers. Figure is taken from a conceptualization in GMS MODFLOW provided by Bergab.

The outcropping bedrock can be seen in figure 4.3. Surrounding the outcrops the recharge zones can be found, seen as dashed zones. These zones are the only locations in the model where recharge is considered to take place, due to impermeable surfaces such as roads and buildings, which generally covers the remaining area. The average annual precipitation was calculated to be 950 mm/year. This number was estimated based on precipitation data between 2017-2020 for Gothenburg (SMHI, n.d). According to Haan et al. (1994), all the precipitation will not become groundwater. The natural groundwater recharge may vary between negligible amounts up to 50 percent depending on the conditions. The lower aquifer is assumed to be in contact with Göta älv, since the wells located at the riverbed and the level in the river largely follows the same fluctuations. Contrarily, Stora Hamnkanalen, which flows through the area, is considered not to be in contact with the lower aquifer due to the fact that the canal is located in the overlying clay layer. The river is therefore considered as a constant locked level, since it influences the wells in connection to the river.

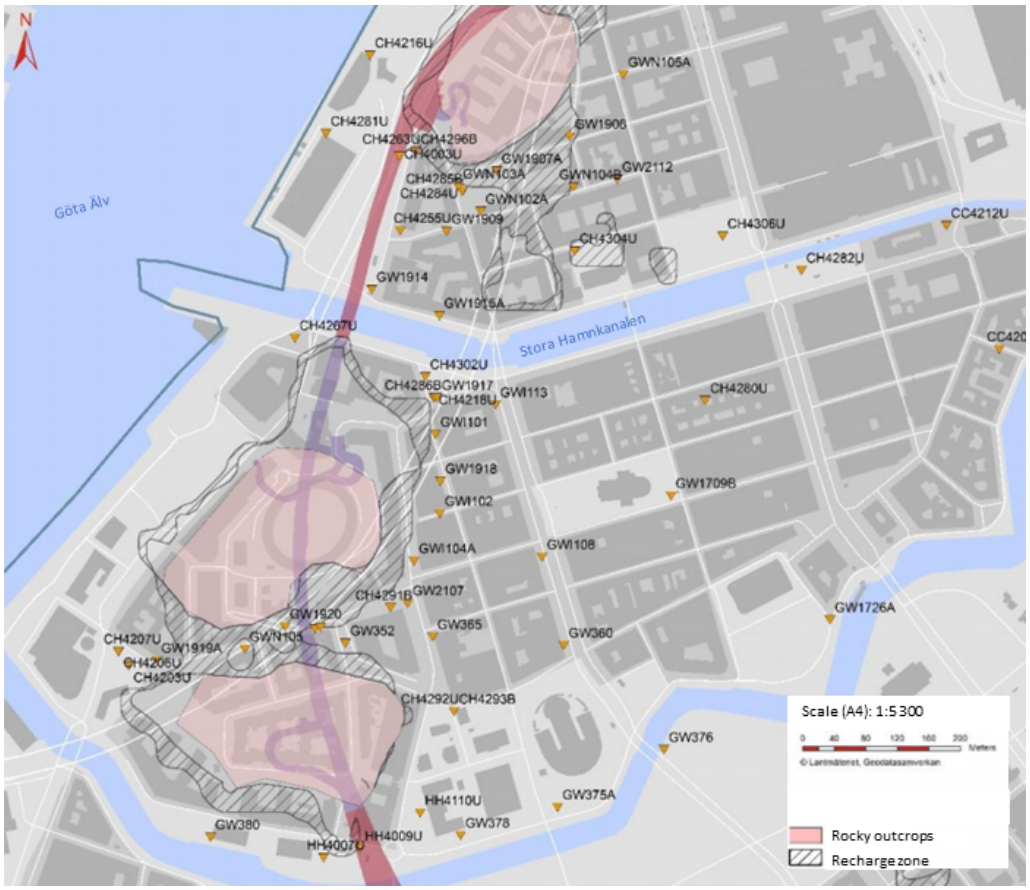

Figure 4.3: Map showing the recharge zones, rocky outcrops and water bodies in connection with the area of study. Modified from Trafikverket (2020).

The figure 4.3 displays the existing Götatunneln, described by two white lines, and Västlänken, seen in red and purple, which will be constructed in the area. As mentioned in the introduction, underground constructions result in water leaking into the tunnel, even though measures such as sealing or grouting have been performed. That is why permanent rock infiltrations in Götatunneln have been installed. Based on data obtained from TMO, which is the Swedish Transport Administration's database with measured data for projects such as Västlänken, a comparison was conducted of the quantities of water leaking into Götatunneln and the quantities of water infiltrated in 2019. The comparison and calculated values can be found in appendix B.1. The comparison showed that the leakage was slightly larger. However, to simplify the models the infiltration have been assumed to equal the leakage into the tunnel, even though this will not be true for all locations in the area.

4.2 Observed infiltration data

As mentioned in chapter 1, four infiltration sites were investigated, two soil infiltrations tests, Hovrätten and Lilla torget, and two permanent rock infiltrations, Göta tunnel IB23 and IB41. These four sites can be seen in figure 4.4, together with three other infiltration sites in Götatunneln, which had to be included in the calibration of the Excel model. The soil infiltrations were only implemented during a limited time frame to investigate the response, while the rock infiltrations are permanently installed to maintain the groundwater levels in the area. The observed infiltration data were gathered from TMO and the reference system used was RH2000. The observation wells chosen for all four infiltrations were spread out geographically in the area, see figure 4.5. However, if data was available, wells were prioritized in the direction of Residenset since this would be of interest in the study. The number of observation wells chosen for each site were governed by the availability of data for that site and time frame. The change in groundwater level in the observation wells were all chosen as close as possible to the actual time frame of the infiltrations. The condition of the observation wells are commented on for all infiltration sites and describes the how quick a change in groundwater level can be observed in the well. Further, the average infiltration flows for the infiltrations were calculated based on volume of water used during the test divided by the time it took to perform the test.

Figure 4.4: The locations of the chosen infiltration wells and boreholes. Eniro (2021)

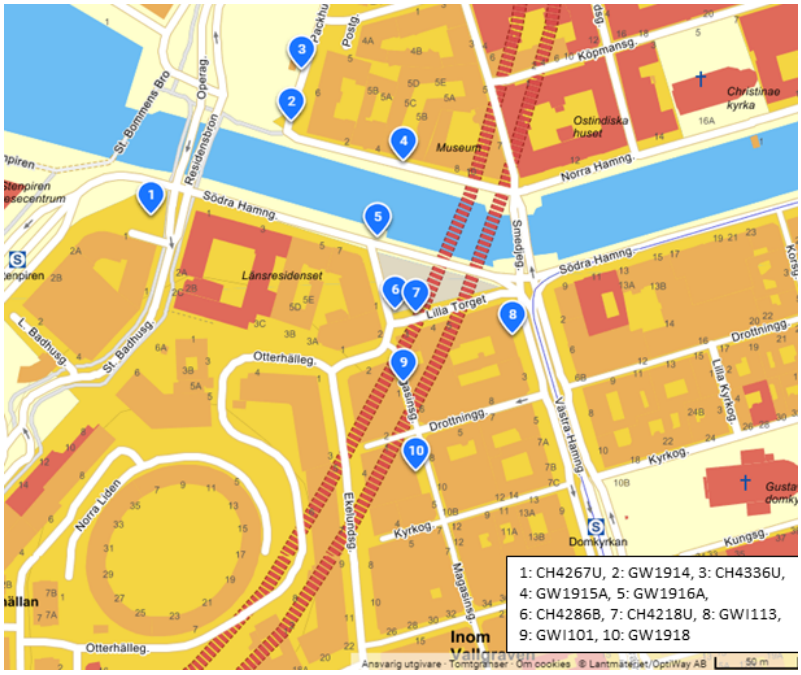

Figure 4.5: The locations of the chosen observation wells. Eniro (2021).

4.2.1 Soil infiltration - Lilla torget

The soil infiltration at Lilla torget took place between the 18th of May 10:10 to the 23rd of May 10:15 2017. Figure 4.4 and 4.5 shows the location of the observation wells and infiltration well. The infiltration well for Lilla torget is called CH4286B and the average flow is 5.45 l/min. Table 4.1 shows information regarding the infiltration well and observation wells. Further, the response, seen from the observed data, generated from the infiltration test was interpreted as poor. However, this location was still chosen to be included in the study, due to it is close proximity to Residenset.

Well ID	Distance from infiltration well [m]	Change in level [m]	Condition
CH4286B	(infiltration well)	2.65	N/A
CH4218U	0.60	2.58	OK, Fast
GWI101	39.90	0.11	OK, Slow
GW1916A	51.42	0.05	Not OK

Table 4.1: Well ID, distance from infiltration well and the change in groundwater level during the infiltration test for the observation wells chosen for Lilla torget.

4.2.2 Soil infiltration - Hovrätten

The soil infiltration at Hovrätten took place between the 7th of March 10:58 to the 9th of March 12:41 2020. Figure 4.5 and 4.4 shows the location of the observation wells and infiltration well, and Table 4.2 lists the distance from infiltration well, change in level and condition of the observation wells. The infiltration well for Hovrätten was CH4337B and the average infiltration flow was 3.68 l/min.

Well ID	Distance from infiltration well [m]	Change in level [m]	Condition
CH4337B	(infiltration well)	2.40	N/A
CH4336U	6.76	1.57	OK, Fast
GW1914	21.23	0.86	OK, Slow
CH4267U	118.05	0.17	OK, Fast
CH4218U	159.3	0.06	OK, Fast

Table 4.2: Well ID, distance from infiltration well and the change in groundwater level during the infiltration test for the observation wells chosen for Hovrätten.

4.2.3 Rock infiltration - Götatunneln

The rock infiltration in Götatunneln is a permanent active infiltration facility. However, there were operational issues with the facility during the fall of 2018 (Trafikverket, 2020). Between the 16th to 27th of November 2018 the last period of operational issue was observed, during which time the infiltration was interrupted. The period directly after the operational issues was therefore chosen, since it shows the response in the surrounding wells when the infiltration facility was later turned on again. The chosen period lasted between the 27th of November 2018 until the end of February 2019, at where it was assumed that the aquifer was in equilibrium again.

In Götatunneln, there are currently six points of infiltration, but only five within the study area, and the whole infiltration facility is controlled by the same pump. In this study two of the infiltration boreholes were investigated, IB23 and IB41. These boreholes were selected both since they are situated in close proximity to Residenset and because the infiltration flow in these boreholes are significantly larger compared to the other boreholes in Götatunneln. Further, figures 4.4 and 4.5 show the location of the infiltration wells and chosen observation wells.

For the calibration model constructed in Excel, five of the infiltration boreholes in Götatunneln were included in the model. In GMS however, only IB23 and IB41 were included, since the other infiltration wells in Götatunneln was not needed for the calibration. This is connected to the assumption that the leakage into Götatunneln is canceled out by the infiltration in the tunnel, mentioned earlier in section 4.1. table 4.3 shows information regarding the infiltration flows and table 4.4 displays the distance from the infiltration well, change in groundwater level in the well and condition about the observation wells.

Infiltration borehole ID	Infiltration flow [l/min]	Direction/Dip angle	Borehole length [m]
IB23	3.06	N110/45	25
IB41	1.65	N95/0	28
IB55	0.055	N180/5	60
IB61	0.40	N140/10	40
IB64	0.26	N185/0	45

Table 4.3: Infiltration borehole ID, infiltration flow, direction, dip angle and length of the borehole for the infiltration boreholes in Götatunneln.

Well ID	Distance from wells (IB23/IB41) [m]	Change in level [m]	Condition
GW1918	88.72/4.64	1.70	OK, Fast
GWI113	49.01/110.60	1.57	OK
CH4286B	21.68/96.32	0.39	N/A
GW1915A	101.40/189.37	0.48	N/A
GW1914	159.11/231.15	0.14	Ok, Slow

Table 4.4: Well ID, distance from infiltration wells and the change in groundwater level during the infiltration test for the observation wells chosen for Götatunneln.

4.2.4 Observed groundwater levels

In GMS MODFLOW the annual average groundwater level had to be used instead of the change in groundwater level, when calibrating the model. Table 4.5 shows the average annual level (RH2000) for all ten observation wells in 2019. This year was selected since no infiltration tests or disruptions were conducted. However, for GW1916A and CH4336U data from 2016-2018 respectively 2020-2021 were used instead, since no data was available in 2019 and an annual average of the available data from these years were used instead.

Observation well	Annual average level [m]
GW1918	3.50
GWI113	1.41
CH4286B	2.04
GW1915A	1.28
GW1914	0.94
GW1916A	1.30
CH4267U	0.29
GWI101	2.93
CH4218U	2.03
CH4336U	1.04

Table 4.5: Annual average groundwater levels for the observation wells used in this study. The reference year used is 2019, for all wells except GW1916A and CH4336U, where an average of several other year were used instead.

4.3 Analytical Calculations

To generate input data different types of analytical calculations were used. These calculations are presented below and will be referred to in the description of models in the following section. The calculated parameters will be presented in chapter 5.

4.3.1 Transmissivity

Transmissivity was calculated by using observed data in section 4.2 for the Cooper-Jacob method (4.1) and Thiem's equation (4.2), for both of the soil infiltration sites. However, due to the lack of continuous data from the rock infiltrations, only Thiem's equation could be used for the infiltrations in Götatunneln.

$$T = \frac{2.3 \cdot \dot{V}}{4\pi \cdot \Delta h_s} \tag{4.1}$$

Where,

T = Transmissivity [m^2/s]
$\dot{V}$ = Abstraction rate [m^3/s]
Δh_s = Change in drawdown over a logarithmic decade [m]

$$T = \frac{\dot{V}}{2\pi \cdot \Delta h_s} \cdot ln\frac{r_2}{r_1} \tag{4.2}$$

Where,

r_1, r_2 = radial distance from pumping well to the observation wells [m]

4.3.2 Radius of influence

In order to determine at which distance no change in water head can be observed, the radius of influence was used. The equation was obtained by rearranging equation (4.2), which then results in equation (4.3). The radius of influence was calculated for each observation well that was used in the separate infiltration models.

$$r_0 = r_1 * \exp\left(\frac{h_1 * 2\pi * T}{\dot{V}}\right) \tag{4.3}$$

Where,

r_0 = Radius of influence [m]

Another method to determine the radius of influence is by plotting the drawdown versus the distance from the pumping well over a period of time (Fetter, 2014; Zheng et al., 2019). Further, by using a linear regression to fit a line to the drawdown data, this results in an estimated radius where the drawdown is equal to zero. Additionally,

a weighted curve was plotted based on observed data and the conditions of the wells, which can be seen in section 4.2. A well defined as fast will show a quick response and will therefore be more reliable when weighting the curve.

4.3.3 Natural groundwater recharge

The natural groundwater recharge was calculated using equations 4.4 and 4.5. This was based on the annual precipitation in Gothenburg, which was described in section 4.1. Noticeable, this approach results in the largest possible natural recharge, but due to soil and surface properties a limited amount of the recharge will actually become groundwater. This aspect will be accounted for later in the models.

$$W = \frac{P_{ave}}{1000 * 24 * 3600} \tag{4.4}$$

$$Q_w = W * A \tag{4.5}$$

Where,

W = Groundwater formation [m/s]
P_{ave} = Precipitation rate [mm/day]
A = Cell area in Excel [m^2]
Qw = Groundwater flow [m^2/s]

4.4 Numerical models

Numerical models are suitable for complex problems, which cannot be solved using analytical equations (Anderson et al., 2015). Instead, numerical methods are used in a iterative process to get approximate answers in order to solve the complex problems. A numerical model generates a solution that is discontinuous in space and time, thus the model uses approximations of flow equations to calculate e.g. the change in head. The purpose of creating the models are that they can give an overall conceptualization of how groundwater moves in soil and rock (Fetter, 2014). This can be difficult to comprehend and create by just observations and calculations. However, it is important to be aware that numerical models includes simplifications and assumptions, and therefore only displays an approximation of the truth. In this thesis, two models were created, Excel and GMS MODFLOW. These models were based on the groundwater flow equation, see equation 4.6, which where solved by the finite difference method, see equation 4.7, which is displayed in the x-direction. (Anderson et al., 2015). However, the practical application of the finite difference method differs between the models since they vary in complexity.

$$\frac{\delta}{\delta x}(K_x\frac{\delta h}{\delta x}) + \frac{\delta}{\delta y}(K_y\frac{\delta h}{\delta y}) + \frac{\delta}{\delta z}(K_z\frac{\delta h}{\delta z}) + W = 0 \tag{4.6}$$

Where,

$K_{x,y,z}$ = Hydraulic conductivity in x,y,z-directions [m/s]
W = Flow input [m^3/s]

$$\frac{\delta h}{\delta x} = \frac{h_{i+1,j,k} - h_{i-1,j,k}}{2\Delta x} \tag{4.7}$$

Where,
Δ = distance between rows, coloumns and layers in x,y,z-directions.
i,j,k = Node indices.

The first model was created in Excel, and is a spreadsheet application in two dimensions. The model only includes one uniform layer which is the friction soil layer. The rocky outcrops in the model were assumed to be impermeable and the friction soil layer was also assumed to be confined both by the clay layer on top and the shallow rock beneath. This type of model is appropriate to use to get an understanding how boundary conditions and hydraulic parameters impact the groundwater level in an aquifer (Gustafson, 2009). Further the Excel model is centered block i.e. the water level in the cell represent the average head in the entire cell.

The second model created with GMS used the MODFLOW algorithm to construct a three dimensional model (Aquaveo, n.d-b). This resulted in a more detailed model with multiple layers and a defined topography. Further, assumptions regarding impermeable outcrops and confined layers made in Excel could be avoided as the approach made it possible to use a more detailed conceptualization. As the GMS MODFLOW model had several layers, groundwater was able to flow in both horizontal and vertical directions (Aquaveo, n.d-a). The multiple layers also generated a three dimensional visualization of the model, where the change in water level could be observed in all layers. Similar to Excel, GMS MODFLOW is a block centered numerical model using the finite-difference method to solve the numerical calculations (Fetter, 2014). The position of the nodes in the grid system is described by indexes i,j and k, which corresponds to rows, columns and layers.

4.4.1 Excel model

Three different Excel models were created, one for each soil infiltration site and one for the rock infiltrations. The first step is to decide the size of the models. The parameter used to determine the size was the radius of influence, since no changes in water level were expected beyond this distance. The result from section 4.3.2 showed a variation in radii, where some results were interpreted to be more accurate compared to other. The size of the model were always chosen to be larger than the average calculated radius of influence and the shape of the model was determined to be quadratic.

The next step was to decided the size of the cells in Excel. The cell size is desired to be as large as possible. However, due to the limitations of Excel and the difficulties to manage and operate a too big model, the grid size was limited to not be more than 40 000 cells. Since the radius of influence varied between the different scenarios, the grid size for each scenario depended on how large the model had to be, thus the cell sizes between models differ, see table 4.6.

Infiltration site	Grid size [Cells]	Cell size [m]
Lilla torget	10 000	2
Hovrätten	10 000	2
Göta tunnel IB23	40 000	3
Göta tunnel IB41	40 000	3

Table 4.6: Name of the models, grid size and cell size for all infiltration models.

The models included three boundary conditions. As previously described, beyond the perimeter no change in water level is expected to occur, based on the result from section 4.3.2. The same boundary condition, no change in water level, is applied for Göta älv according to 4.1. In Excel, this constant locked level boundary was applied by setting the cell values at the perimeter equal to zero i.e. no change in water head, see figure 4.6.

The second boundary condition was applied around the rocky outcrops since these were assumed to be impermeable, which is not the case in reality. Impermeable boundaries in Excel means that the gradient over the boundary is equal to zero, which is achieved by mirroring the cell situated next to it, see figure 4.6. The third boundary condition in the models were applied for the recharge zones. The recharge in the model was based on the calculations performed in section 4.3.3. The amount of natural groundwater recharge actually reaching the aquifer is calibrated based on the range presented in section 4.1.

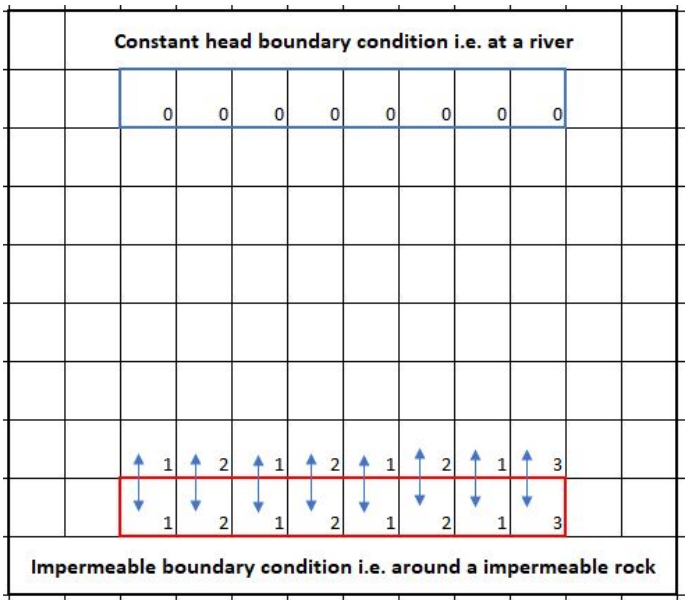

Figure 4.6: The boundary conditions and how they are applied in the Excel models.

The locations of the observation and infiltration wells can be seen in figures 4.5 and 4.4. The cells in the model were ascribed with different equations depending on whether the cell had any new input, connected to infiltration wells or recharge zones, or if the cell value only depended on adjacent cells (Gustafson, 2009). For a cell that is only impacted by adjacent cells, equation (4.8) was used. This equation is called the difference star without a source term and is derived from equation 4.7. The principle is displayed in figure 4.7.

$$h_0 = \frac{h_1 + h_2 + h_3 + h_4}{4} \tag{4.8}$$

Where,

$h_{1,2,3,4}$ = Water level in adjacent cells [m]

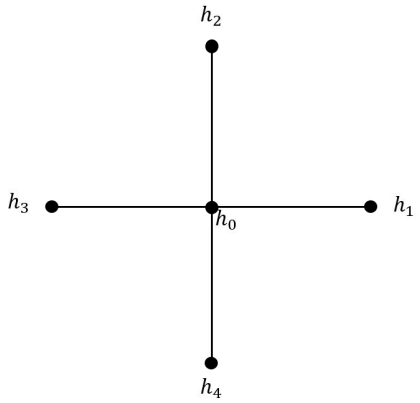

Figure 4.7: The principle of the difference star without a source term. Modified from Gustafson (2009).

For cells which were located in the recharge zones or when a general transmissivity were used for a well, equation 4.8 was applied, but with an additional term for the source. This resulted in a difference star equation with a source term, see equation 4.9 (Gustafson, 2009). The transmissivity value used for the recharge zones and Göta tunnel IB55, IB61 and IB64, where the regional transmissivity value listed in table 3.1. Further, for Göta tunnel IB41 the same equation was applied but instead of the regional transmissivity an average value of the calculated transmissivities, seen in section 4.3.1, was used.

$$h_0 = \frac{h_1 + h_2 + h_3 + h_4 + \frac{W * \Delta^2}{T}}{4} \tag{4.9}$$

Where,

W = Groundwater formation [m/s]
Δ = Area of the cell [m^2]
T = Transmissivity [m^2/s]

For the remaining wells i.e. Lilla torget, Hovrätten and Göta tunnel IB23, a modified version of equation 4.9 was used, see equation 4.10. This version of the difference star equation accounts for different transmissivities in varying directions, see figure 4.8 (Gustafson & Svensson, 1994). The reason why this version could not be used for Göta tunnel IB41, was because transmissivities could not be calculated in different directions.

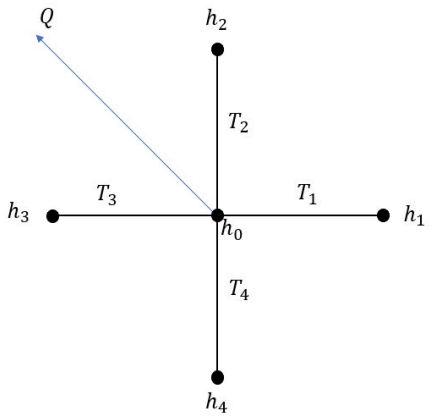

Figure 4.8: The modified difference star accounting for different transmissivities in varying directions. Modified from Gustafson and Svensson (1994).

.

$$h_0 = \frac{h_1 * T_1 + h_2 * T_2 + h_3 * T_3 + h_4 * T_4 + Q}{T_1 + T_2 + T_3 + T_4} \tag{4.10}$$

Where,

Q = Infiltration flow [m^3/s]
$T_{1,2,3,4}$ = Transmissivity [m^2/s]

Table 4.7 shows which wells that were used for each infiltration and in which direction they are located. For some wells it was not possible to evaluate the transmissivity, since no observation well with reliable data were located in that direction.

Infiltration site	North	East	South	West
Lilla torget-CH4286B	GW1916A	CH4218U	GWI101	Ave
Hovrätten-CH4337B	CH4336U	CH4218U	GW1914	CH4267U
Göta tunnel IB23	GW1915A	GWI113	GW1918	Ave (N/S)
Göta tunnel IB41	Ave	Ave	Ave	Ave

Table 4.7: Displays which well that was used in each direction for each infiltration. Cells marked with Ave (N/S) refers to the average value of the transmissivities in the north and south directions, and Ave refers to the average of all calculated transmissivities.

After this step, the procedure between the soil and rock models diverge due to different setups. Since both soil infiltrations only had one infiltration well in each model the iteration process could start immediately after all the input values were inserted. The models were iterated until steady state, which was decided to be achieved when the water levels in the wells were not changing more than 0.001 meter. When steady state was achieved the models were calibrated. The purpose of the calibration was to achieve the same order of magnitude for the modelled change in water level and the measured water level in the observation wells, see section 4.2. This implied that the modelled values did not have to be exactly the same as the measured values. The parameters that could be adjusted in the calibration are listed below.

1. Alternate between the two transmissivity values, calculated by Thiem's equation 4.2 and Cooper-Jacob equation 4.1, in all directions.
2. It was determined that the recharge zones could vary between 0-50 percent of the total calculated natural groundwater recharge, based on section 4.1. Notice that the individual recharge zone must be consistent and have the same percentage in all Excel models.

For the rock infiltration, both Göta tunnel IB23 and IB41 operate together with the rest of the infiltration boreholes in the Göta tunnel (IB55, IB61, IB64) and are supplied by the same pump. Consequently, a different procedure had to be implemented for the rock infiltrations. When the infiltration flow, length and direction for all boreholes were inserted in the model, a calibration model was created to recreate the observed values. This was done in order to separate the individual responses for each borehole, since they are controlled by the same pump. Data on the boreholes can be found in section 4.2.3. For this model the same assumptions on steady state and the correct order of magnitude in the wells compared to the observed data, used in the soil infiltration, were applied. When calibrating the rock model the following parameters could be adjusted.

1. Same as number two for soil infiltration.
2. The amount of cells assigned a flow term was increased in E-W due to the previously described dominant fracture pattern. 4.1.

When the calibration model had achieved steady state and the correct magnitude of the change in head in the observation wells, only one of the simulated boreholes (Göta tunnel IB23 and IB41) was used at a time. This was done in order to to get the response from a single borehole.

4.4.2 GMS MODFLOW model

In GMS MODFLOW, the geological conceptualization of the studied area can be seen in figure 4.2, and the model is provided by Bergab. The model includes five layers; bedrock, shallow rock, friction soil, clay and fill material. The conceptualization is based on TINs which describe the elevation array of an area, which in turn have been used to create the solids shown in the figure 4.2 (Aquaveo, 2017). TIN stands for triangulated irregular network and is described by a set of triangles that together form a surface. Further, TINs can be translated into a solid model, where the solids in between the TIN-layer form 3D shapes. When creating the solids interpolation errors occurred and the command "truncate to bedrock" was used. This command assumes that the base elevation of the bottom layer equals the top of the cell representing the bedrock.

As opposed to the Excel model, in GMS MODFLOW hydraulic conductivity values had to be set for the friction soil, as performed in Excel, but also for the other four remaining layers. The values from these four layers where found in literature and from borehole investigations performed in the area, see section 3. The hydraulic conductivity values are presented within a range, which were later used when calibrating the model. The values can be found in table 4.8. The hydraulic conductivity in the friction soil will be calculated by using equation 4.11 and displayed in chapter 5. The average thickness of the friction soil is based on the figure 4.2, and is assumed to be 2 m.

$$T = K * b \tag{4.11}$$

Where,

T = Transmissivity [m^2/s]
K = Hydraulic conductivity [m/s]
b = Thickness of aquifer [m]

Since, the formation and deposition of rock and soil results in anisotropic characteristics, it is of interest to define the variations in hydraulic conductivity in horizontal and vertical directions. The ratio of the hydraulic conductivity in horizontal and vertical directions are proportional to the anisotropy. However, due to the lack of data discussing anisotropy in the studied area, the value were assumed to be one, assuming a homogeneous material. Consequently this results in that the vertical hydraulic conductivity will equal the horizontal hydraulic conductivity, since they are proportional to the vertical anisotropy (Hölting & Coldewey, 2019). The NWT (The Newton package) solver was picked for the models (Aquaveo, 2011). This solver was chosen since it better handles drying and rewetting of cells and therefore may help the model to converge. Further, this results in that the UPW (Upstream weighting) package was selected by default to describe the material properties using Material ID:s in GMS MODFLOW.

	Fill material	Clay	Shallow rock	Bedrock
K_h [m/s]	1E-06 - 1E-04[1]	1E-09-1E-06[2]	1E-07 - 2E-06[3]	1E-08 - 2E-07[4]

Table 4.8: Chosen conductivity values for GMS MODFLOW for fill material, clay, shallow rock and bedrock [1]Trafikverket, 2016c, [2]Fetter, 2014, [3]Trafikverket, 2016b and [4]Trafikverket, 2016b.

Since the model was much larger than what was needed in this study, it had to be cut to the appropriate size. In GMS MODFLOW, one model was constructed for all infiltration tests, and the size of the model was decided to be larger than the maximum radius of influence used in Excel. Further, the size of each cell also had to be decided. The cell size was governed by the fact that using too few cells results in less accurate results and using too many leads to difficulties making the program converge into a solution. Consequently the chosen cell size was approximately 10 meters in x-direction and 13 meters in y-direction.

The boundary conditions were chosen to be similar to the ones in Excel, and are described in depth in section 4.1. Around the model a constant head of zero was set, to simulate similar boundary conditions as chosen for Excel. This is a simplification of the reality since the groundwater levels vary in the area. However, in order to be able to make a just comparison between the models, these assumptions had to be made. Further, the recharge zones were created, having the same shape as seen in figure 4.3 and calculated using equation 4.5. In GMS MODFLOW a drainage element was also created, to avoid large amounts of water piling up. The drainage arcs were located along Göta älv and Stora Hamnkanalen, to simulate naturally occurring surface discharge to the water bodies. For the drainage element, a conductance value had to be assumed, which can be seen in equation 4.12 (Aquaveo, 2019).

$$C_{arc} = \frac{K}{t} w \tag{4.12}$$

Where,
C_{arc} = Conductance [m/s]
K = Hydraulic conductivity [m/s]
w = Width of the material along the arc [m]
t = Thickness of the material [m]

This value assumed a ratio between the length and height of the water bodies to be two and used the hydraulic conductivity for the fill material. This value was assumed to be uniform over the length of the arc and the drainage arcs followed the elevation of the top surface.

Finally the observation wells were also added to the model, and the level in each well can be found in table 4.5. The constant head boundary, recharge zones, drainage and location of observation points can be seen in figure 4.9. The model was then calibrated by changing the hydraulic conductivity. The conductivity values were changed within the ranges presented in table 4.8 and for the hydraulic conductivity in friction soil, the values were altered between the minimum and maximum values calculated using Thiem's equation and Cooper-Jacob method, see section 4.3.1.

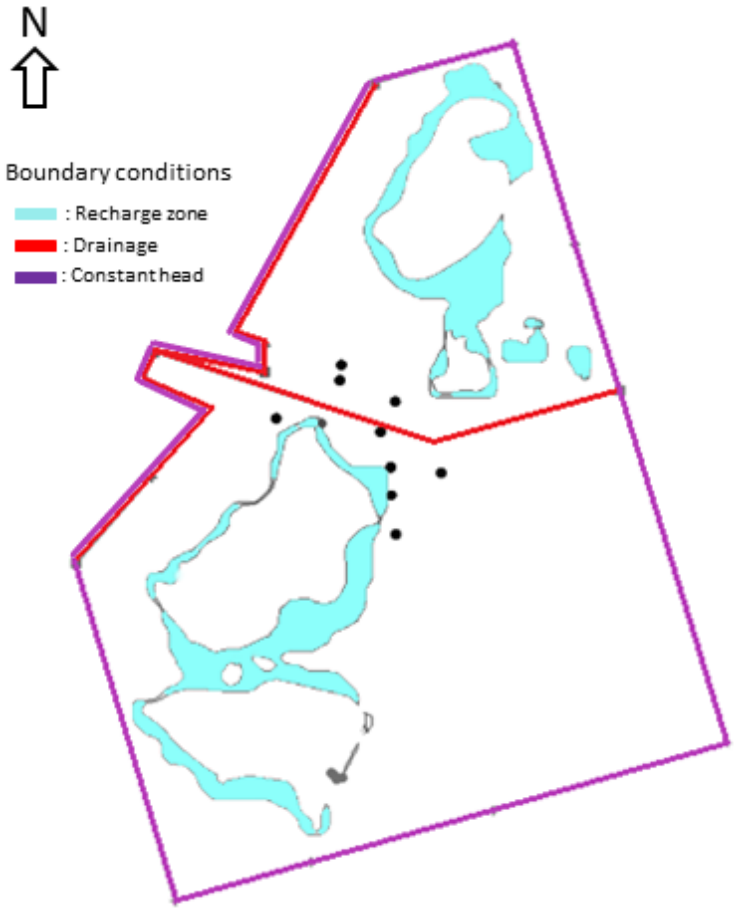

Figure 4.9: The boundary conditions chosen for the model, including drainage, constant head and recharge. The black dots shows the location of the observation wells.

After the model was calibrated, the infiltration wells were included in separate models. The same flow and location were chosen as described in the observed data, see section 4.2. The WEL package was used to include the wells. This package includes vertical wells, where the coordinates and abstraction rate has to be defined (Aquaveo, 2018). In soil the wells were added as single points, to simulate a point source. However, in rock the infiltration flow was equally divided over the entire length of the borehole plus two additional cells to simulate the fractures in E-W.

Another alteration that was made was that the borehole was only placed in the shallow rock, and not in the underlying bedrock as it is in reality. This was done since the model does not include any fractures which is the dominant flow path in crystalline rock, described in section 2.1. After the simulation had converged in GMS MODFLOW, a response curve and a plot showing the change in head were created for each infiltration.

5
Results

This chapter displays the results from the Excel and GMS MODFLOW modelling. Further, to construct the models, the transmissivity values and radius of influence had to be calculated beforehand, and can be seen in this chapter. Finally, the modelled data, change in head plots and response curves have been constructed to show how the change in groundwater levels propagate depending on the type of infiltration and location.

5.1 Analytical calculations

This section shows the result from the analytical calculations and displays the values chosen in the models. All the calculated parameters can be seen in appendices C.1.1 and C.1.2

5.1.1 Transmissivity

In table 5.1 the applied transmissivities for all infiltrations in Excel can be found. The table also includes in which direction the transmissivity was assigned. All calculated transmissivity values can be found in appendix C.1.1.

Infiltration site	North, T [m^2/s]	East, T [m^2/s]	South, T [m^2/s]	West, T [m^2/s]
Lilla torget-CH4286B	3.47E-05	3.68E-04	3.41E-05	1.45E-04
Hovrätten-CH4337B	5.61E-05	4.03E-05	1.87E-05	4.92E-06
Göta tunnel-IB23	1.02E-04	4.14E-06	6.44E-06	5.46E-05
Göta tunnel-IB41	2.60E-05	2.60E-05	2.60E-05	2.60E-05

Table 5.1: The chosen Transmissivity values [m^2/s], which were applied in each direction for the different infiltration scenarios.

5.1.2 Radius of influence

In this section, the calculated radius of influence values are displayed. Table 5.2 shows the influence radius which were applied in the different models. Further, all influence radii can be found in appendix C.1.2.

Infiltration site	Radius of influence [m]
Lilla torget-CH4286B	100
Hovrätten-CH4337B	108
Göta tunnel-IB23	300
Göta tunnel-IB41	300

Table 5.2: The chosen influence radii for all the infiltration models [m].

5.1.3 Natural groundwater recharge

The natural recharge was calculated using equation 4.3.3 and used the values of precipitation listed in section 4.1. The number was calculated to be 3.015*E-08 m/s.

5.2 Excel models

In figure 5.1, the propagation of infiltrated water from the soil infiltrations at Lilla torget and Hovrätten are displayed. Further, figure 5.2 shows the propagation generated from the rock infiltrations in Götatunneln. In both figures observation wells are numbered for each infiltration scenario. Further, the calibration of the models resulted in that the recharge zones north of Stora Hamnkanalen were set to 20 percent of the total amount of the calculated natural recharge, see section 5.1.3, and the recharge zones south of Stora Hamnkanalen was set to 5 percent.

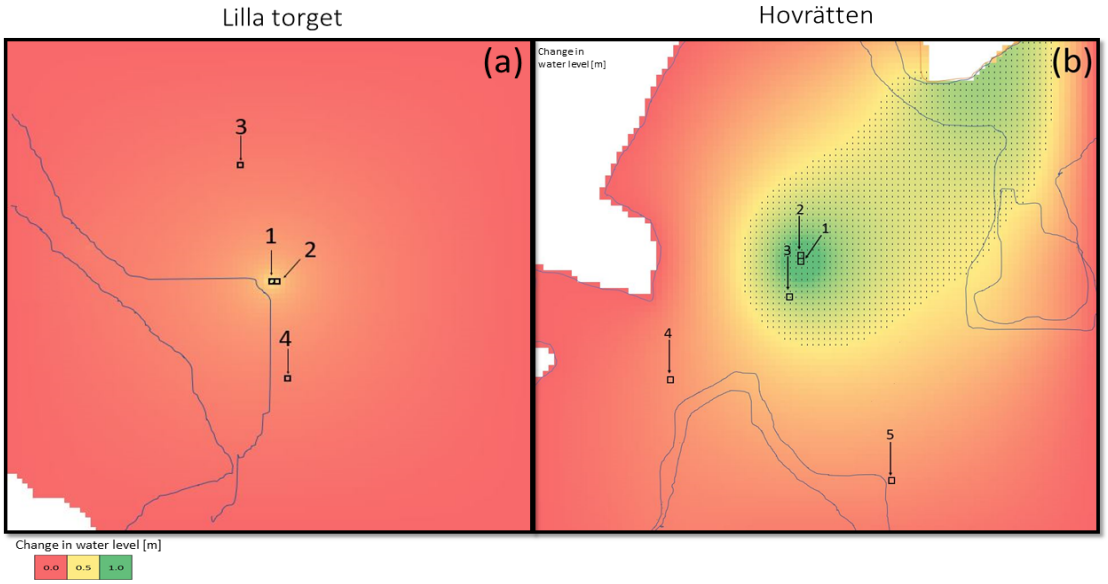

Figure 5.1: The propagation obtained from the soil infiltrations at (a) Lilla torget and (b) Hovrätten. Displayed wells in (a); 1: CH4286B, 2: CH4218U, 3: GW1916A, 4: GWI101. Displayed wells in (b): 1:CH4337B, 2: CH4336U, 3:GW1914, 4:CH4267U, 5: CH4218U.

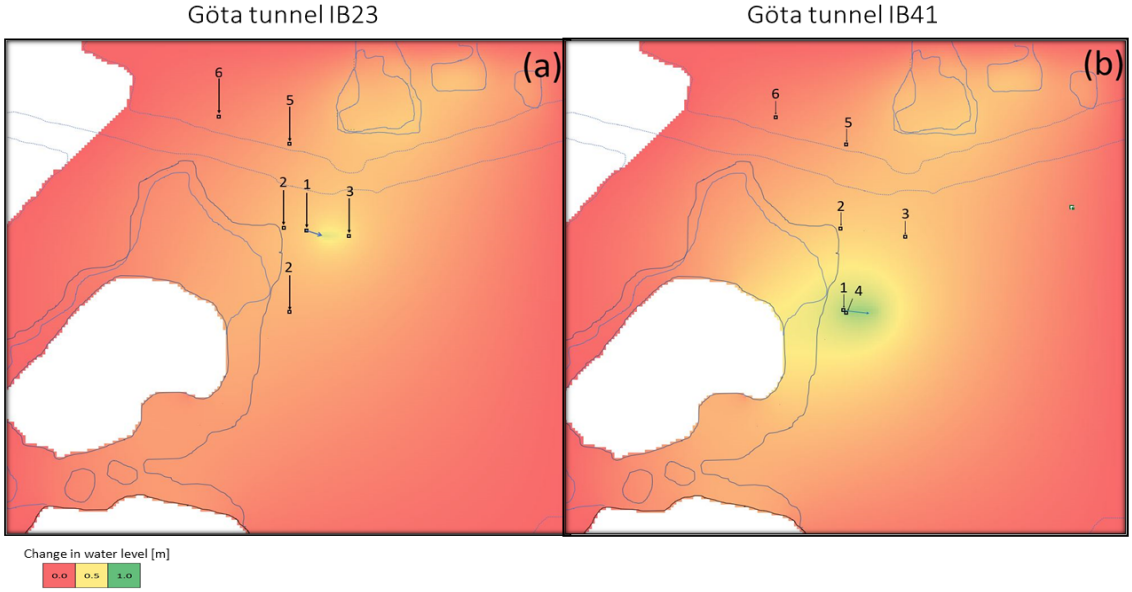

Figure 5.2: The propagation obtained from the rock infiltrations at (a) Göta tunnel IB23 and (b) Göta tunnel IB41. Displayed wells in (a); 1: IB23, 2: CH4286B, 3:GWI113, 4: GW1918, GW1915A, GW1914. Displayed wells in (b); 1: IB41, the rest are the same as in (a).

In order to compare the obtained responses between the different models, the change in head vs. the distance from the infiltration points can be seen in figure 5.3. Since Residenset is of interest, an approximate direction towards the risk object was used. Given that the infiltration flows vary between the different infiltrations, a normalization of the maximum and minimum change in water level was performed. The normalization of the change in head plotted against the distance can be seen in figure 5.4.

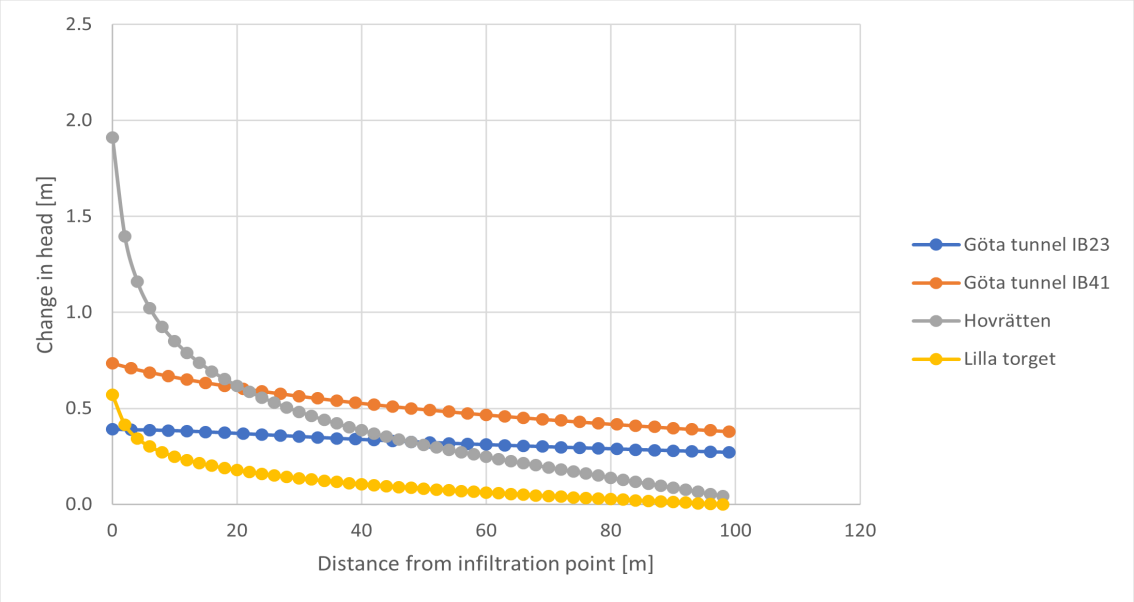

Figure 5.3: Change in head [m] vs. the distance from the infiltration point [m] for Hovrätten, Lilla Torget, IB23 and IB41 in Excel.

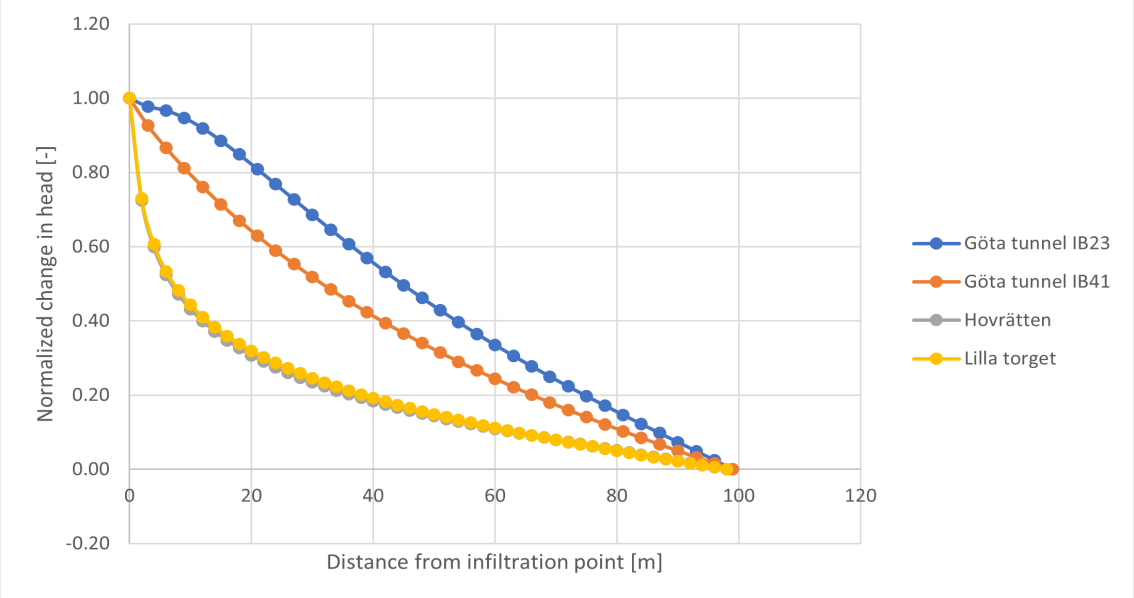

Figure 5.4: Normalized change in head [m] vs. the distance from the infiltration point [m] for Hovrätten, Lilla Torget, IB23 and IB41 in Excel.

5.3 GMS MODFLOW model

The chosen hydraulic conductivity values used in GMS MODFLOW, can be seen in table 5.3. They have been chosen within the ranges presented in table 4.8, when calibrating the model against the measured groundwater levels. To get a range of the hydraulic conductivity in the friction soil the smallest and largest transmissivity values, seen in section C.1.1, were chosen. These values where 6.4E-06 m^2/s and 3.68E-04 m^2/s. Further, to get the hydraulic conductivity, an average thickness of 2 m was assumed for the friction soil and equation 4.11 was used to calculate the hydraulic conductivities. The range was calculated to be from 3.2E-06 m/s to1.84E-04 m/s, and these values where seen as the lower and upper limit when calibrating the model and choosing the final conductivity value for the model.

	Fill material	Clay	Friction soil	Surface rock	Bedrock
K_h [m/s]	1.0E-05	1.0E-07	3.0E-05	1.0E-06	1.0E-08

Table 5.3: Chosen conductivity values in GMS MODFLOW for all five layers after calibrating the base model.

The calibrated base model can be seen in figure 5.5. The model was calibrated to be within one standard deviation from the observed groundwater levels. The value chosen for the recharge can be seen in section 5.1.3 and the value chosen for the conductance was 0.0004 m/s, and this was based on the assumptions presented in section 4.4.2.

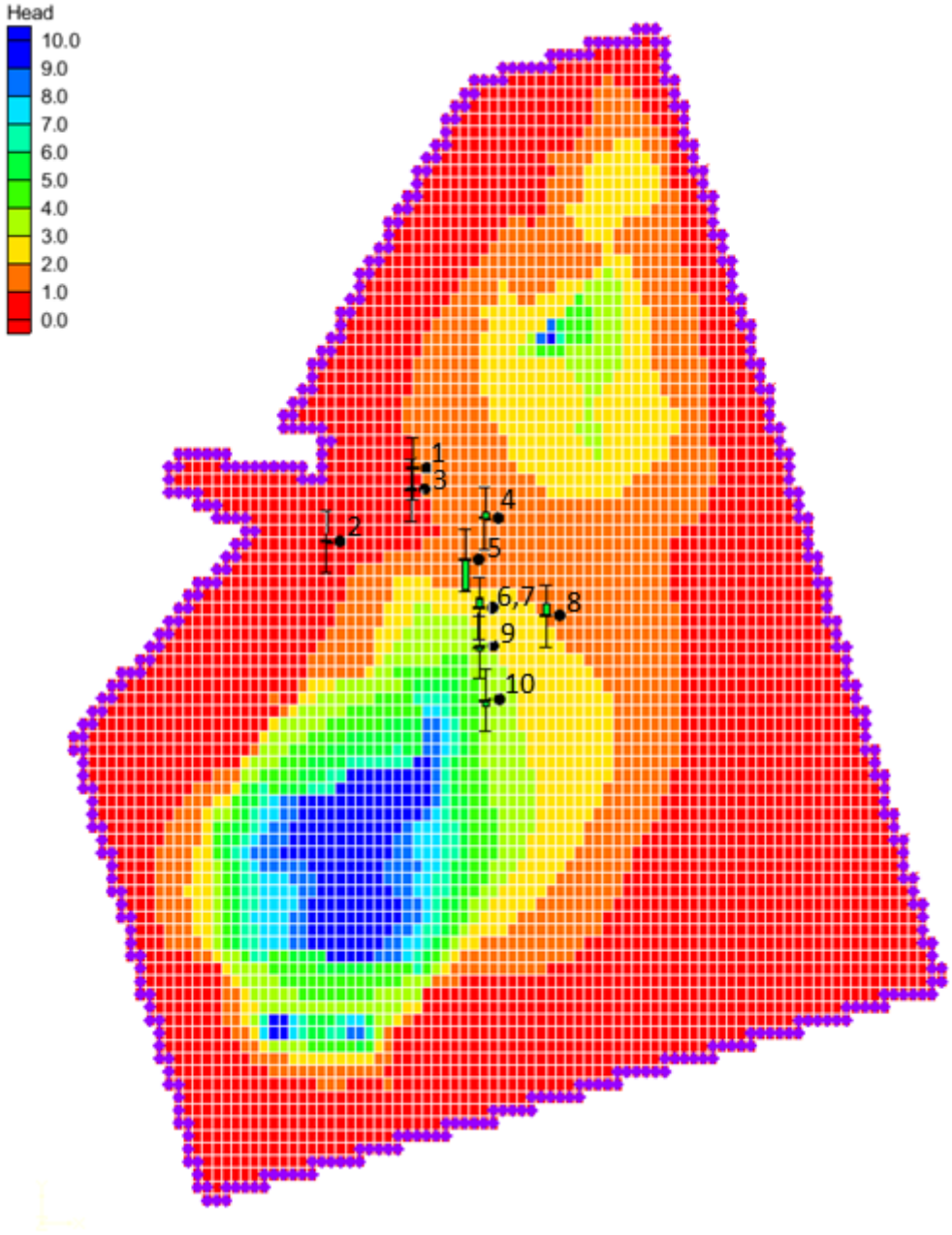

Figure 5.5: Groundwater levels [m] in the studied friction soil layer for the base model. The model was calibrated to be within one standard deviation of the measured groundwater levels. Numbered observation wells: 1-CH4336U, 2-CH4267U, 3-GW1914, 4-GW1915A, 5-GW1916A, 6-CH4218U, 7-CH2486B, 8-GWI113, 9-GWI101, 10-GW1918.

Figures 5.6 and 5.7 show the responses of the infiltrations in soil respectively rock, displayed as change in head. The modelled soil layer is the friction soil layer. The observation wells in the models can be seen as grey dots, and are the same as the ones in the base model. The Change in head legend varies from 0-1 meters where red represents one meter and blue represents 0 meters.

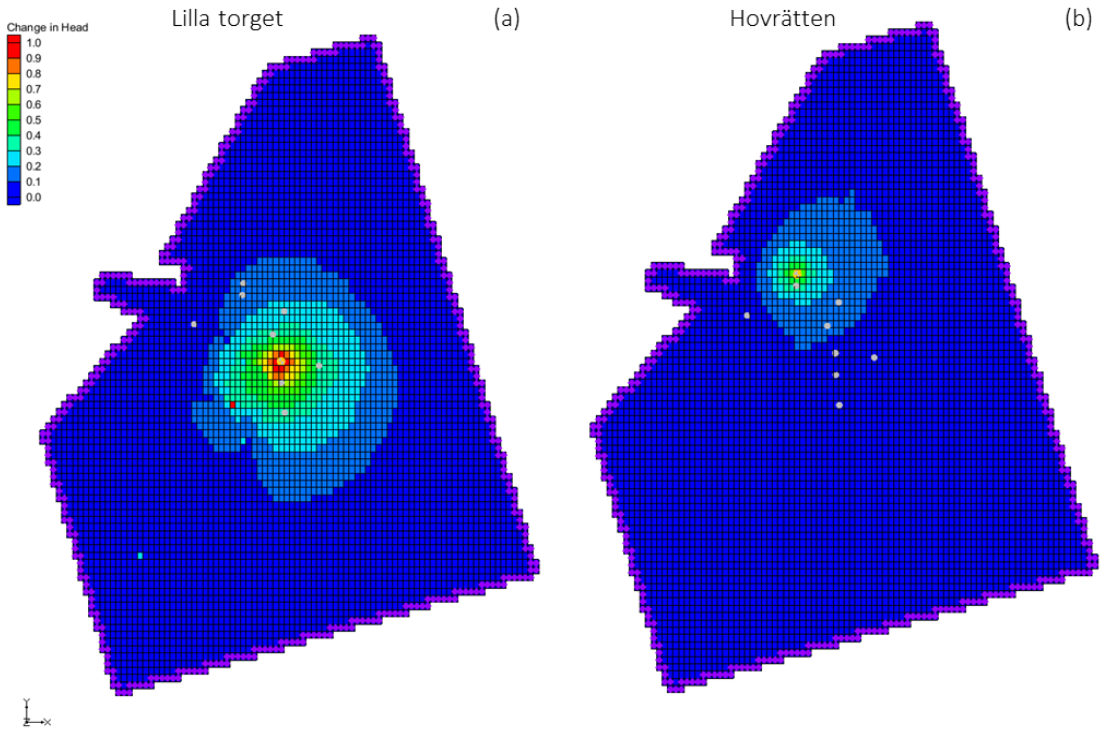

Figure 5.6: Change in Head [m] responses for the soil infiltration at (a) Lilla torget and (b) Hovrätten.

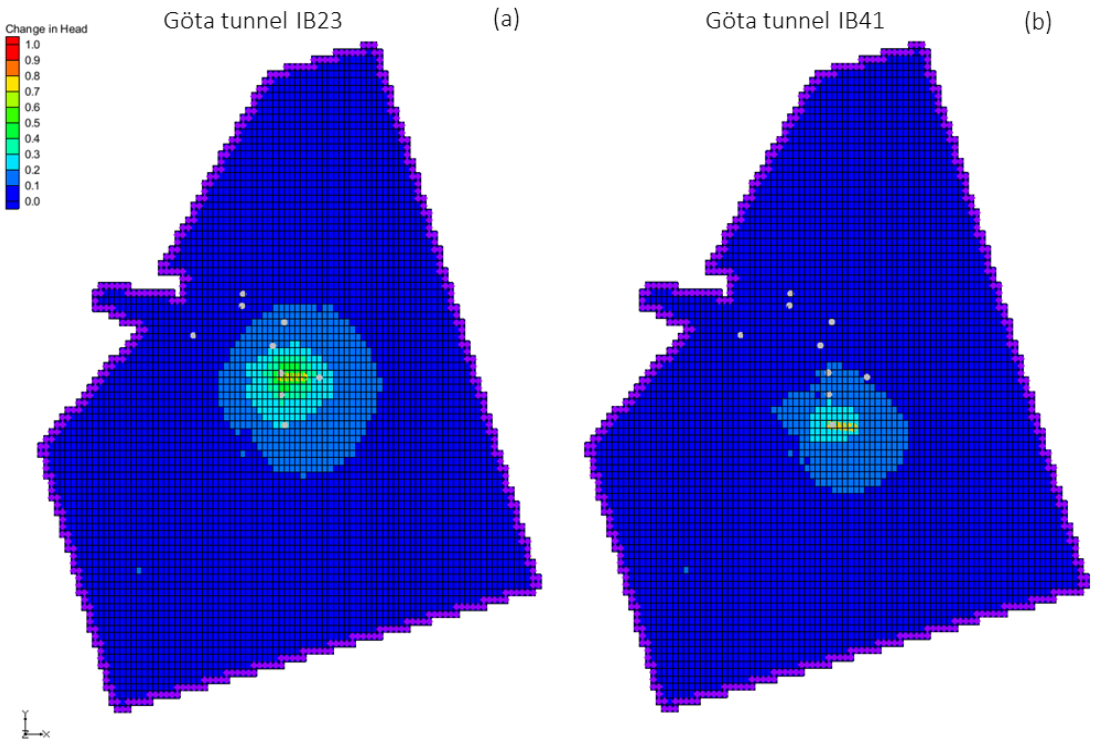

Figure 5.7: Change in Head [m] responses for the bedrock infiltration at (a) Götatunnel IB23 and (b) Götatunnel IB41.

Figure 5.8 shows the change in head versus the distance from the infiltration point for all four infiltration sites. Additionally, figure 5.9 shows the normalized change in head versus the distance from the infiltration point. The direction of the responses is taken to be arbitrarily in the orientation towards Residenset and the distance of the responses is taken to be approximately 100 meters. These conditions are the same as chosen for the Excel models.

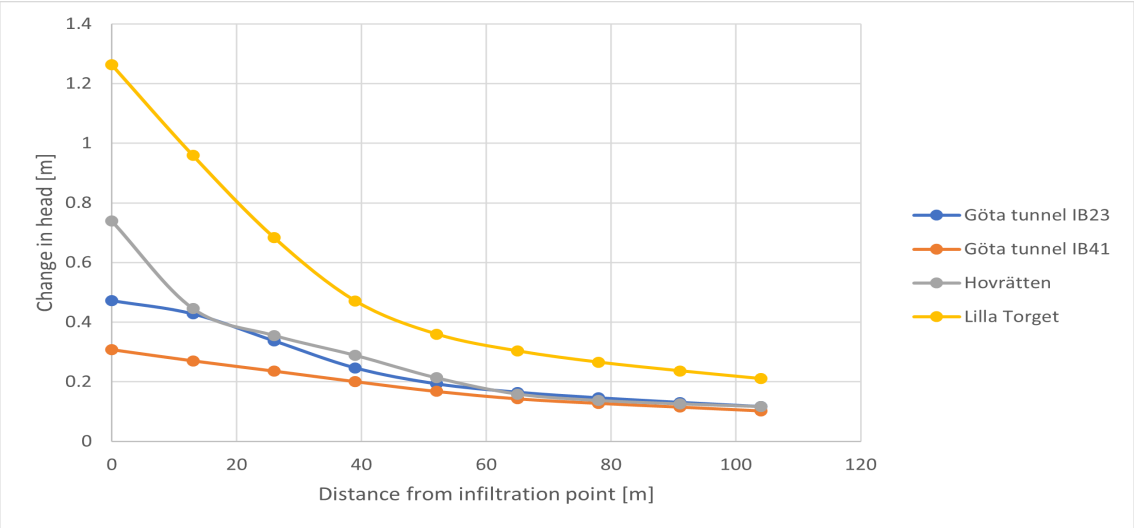

Figure 5.8: Change in head [m] vs. the distance from the infiltration point [m] for Hovrätten, Lilla Torget, IB23 and IB41 in MODFLOW.

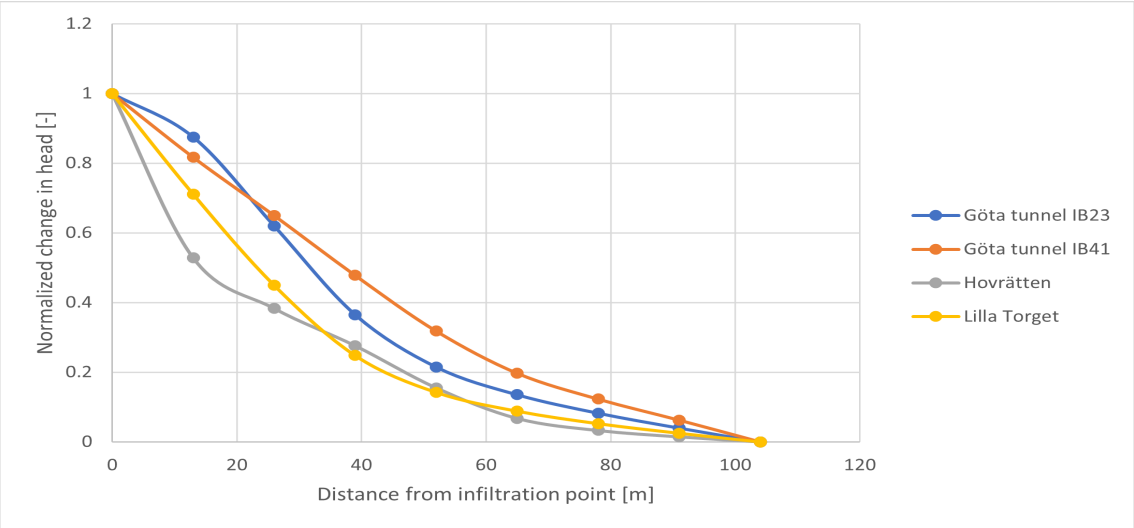

Figure 5.9: Normalized change in head [m] vs. the distance from the infiltration point [m] for Hovrätten, Lilla Torget, IB23 and IB41 in MODFLOW.

5.4 Modelled data vs. Observed data

The modelled and observed change in groundwater level can be seen in figure 5.10. The graphs show how well the models were able to recreate the measured values. As displayed in the figure, the results from Excel correlates better the observed change in water level compared to the results obtained from GMS MODFLOW. This can also be seen in table 5.4, which shows the Spearman rank order correlation coefficient for all simulations (Iversen & Gergen, 1997).

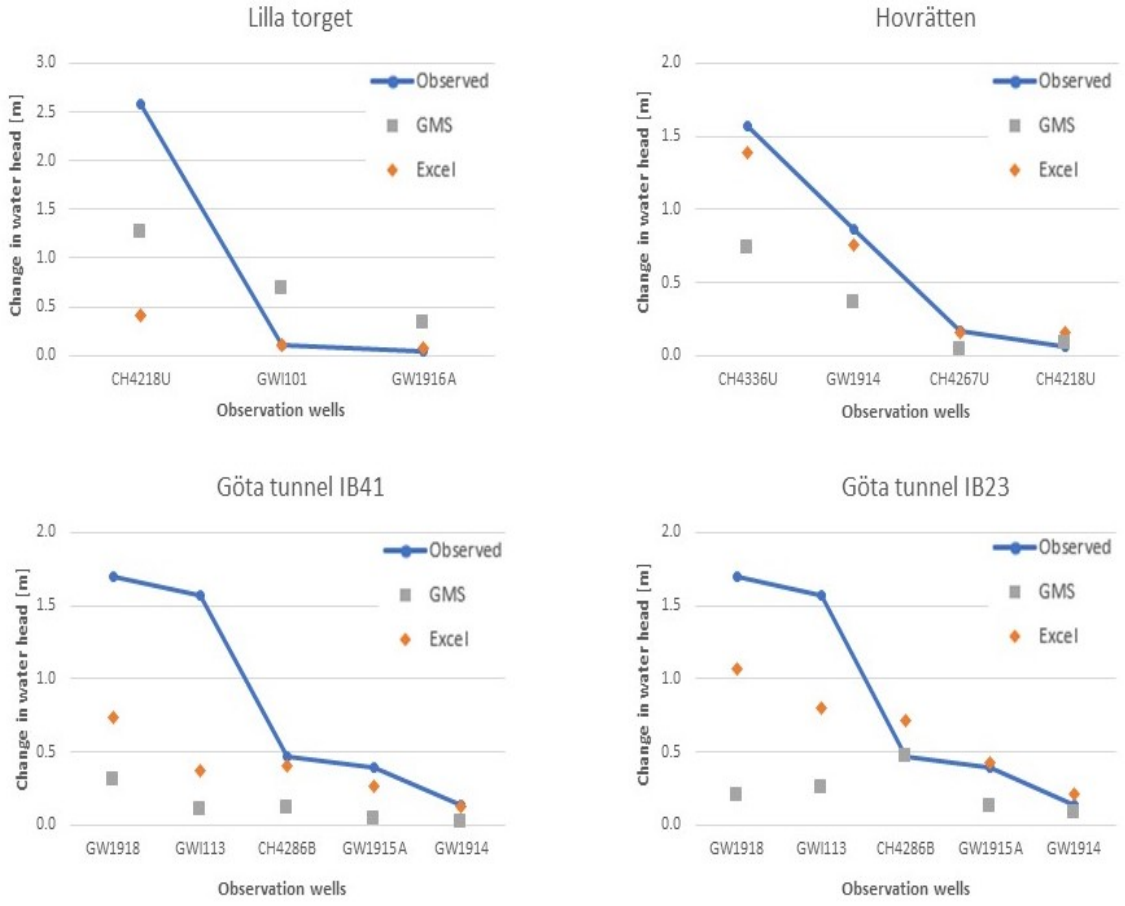

Figure 5.10: The modelled and observed change in water level [m] due to the infiltrations.

Infiltration site	GMS MODFLOW Correlation Coefficient [-]	Excel Correlation Coefficient [-]
Lilla torget	1.0	1.0
Hovrätten	0.8	1.0
Göta tunnel IB41	0.6	1.0
Göta tunnel IB23	0.9	1.0

Table 5.4: The Spearman correlation coefficient for all infiltration sites.

6
Discussion

This chapter discusses the results obtained in chapter 5. The discussion is divided into three parts; rock and soil responses, comparison of Excel and GMS MODFLOW, and suggested infiltration at Residenset. Further, it is important to bear in mind that the results generated in this study are site specific, since the results have not been compared with similar studies due to a lack of comparable literature. Therefore, different results can be obtained for other sites with different hydrogeological conditions.

6.1 Rock and soil infiltrations

Figures 5.9 and 5.4, show the normalized graphs of the change in head versus distance from the infiltration well, in GMS MODFLOW and Excel. What can be seen in both graphs are that the rock infiltrations (Göta tunnel IB23 and IB41) tend to be more linear compared to the soil infiltration (Hovrätten and Lilla torget). The soil infiltrations display a quicker drop in the graph between the first and second measuring point, and the response shows an exponential trend in soil. Further, figure 5.3, which shows the non-normalized change in head versus distance from the infiltration point in Excel, displays that 100 meters away from the infiltration point the rock infiltration shows greater response compared to the soil infiltration. This response corresponds with the observed data which shows that the rock infiltration is more diffusive and that the fractures in the rock enables the water to flow further away from the infiltration point. However in figure 5.8, which is the corresponding graph in GMS MODFLOW, this pattern does not exist and the soil infiltrations show greater or equal response in the surrounding area compared to the rock infiltrations. One possible explanation is that the GMS MODFLOW model is affected by the location and depth of the infiltration point to a greater extent compared to the Excel model as the GMS MODFLOW model has multiple layers with a variation in thicknesses. Further, the GMS MODFLOW model seems to be correlated to the infiltration flow to a greater extent compared to the Excel model.

The magnitude of the maximum infiltration pressure is limited by local conditions and varies between rock and soil. For grouting practices in rock, a recommendation is that the maximum pressure used is limited by the depth of the fractures and the state of the rock (Rafi, 2014). In Sweden, a general practice can be considered to be around 1 bar/meter of depth, and varying around this number based on the condition of the rock. This practice is used to prevent jacking, which is when the

rock mass is lifted due to the increased water pressure. For soil, if the pressure is too great piping can occur, which is when channels are formed within the soil which can occur due to high pore water pressures (Ojha et al., 2003). A limiting factor is the amount of clay overlying the friction soil and it controls the pressure which can be applied when infiltrating water. Contrary, a too low pressure may cause clogging, described in section 2.2. Consequently, this results in that the capacity of the well itself is limiting and not the infiltration flow. The capacity of the well is connected to the site specific conditions. Depending on for example the thickness of the friction soil or to which extent the lower aquifer is connected, the response from a infiltration facility can vary. For infiltrations in rock, the connectivity of the fractures play a great role, as mentioned in section 2.3, and also knowledge about the heterogeneity of the rock.

6.2 Excel and GMS MODFLOW models

As mentioned, in this study two model approaches were created in order to both be able to validate results, but also to determine how the prerequisites of the models affects the results. The Excel model is easier to both comprehend and structure, as basic assumptions and simplifications can be applied more conveniently, thus less time was needed to create the models (Ankor & Tyler, 2019). However, GMS MODFLOW was created with parameters such as multiple layers, topography and vertical flows, which all were neglected in the Excel model. Further, these parameters results in that the confining clay layer are not completely impermeable, and the estimation of natural recharge for each recharge zone could be omitted. As the purpose of this study was to compare rock and soil infiltrations similar conditions, inputs and assumptions were desirable. In GMS MODFLOW more assumptions were needed to be made, since the model includes more degree of freedom compared to Excel. This resulted in that it was difficult to implement similar settings in the models, and consequently, a fair comparison between the models were more challenging to conduct.

An interesting point regarding the model approaches are whether the GMS MODFLOW model have accomplished more reliable results compared to the Excel model. The results in table 5.10, show that the observed changes correlate better with the responses obtained from Excel, in comparison to GMS MODFLOW. A possible reason why the observed response are reflected better in Excel could be that the cell size in GMS MODFLOW was larger. Since the finite difference method is center blocked, the average change in head is applied over the whole cell area, thus local peaks and lows in water level are left out. Another interesting result in table 5.10, is that the response at Lilla torget is the highest in GMS MODFLOW but the lowest in Excel. As mentioned GMS MODFLOW accounts for topography which can increase the propagation for infiltrations located at higher altitude, e.g. at Lilla torget, as water naturally strives to equalize pressure differences. Further, in GMS MODFLOW the rock infiltrations are placed in the shallow rock compared to Excel were the infiltrations are spread out in the friction soil layer according to the inter-

preted fracture mapping. In table 5.10, the results from GMS MODFLOW is much lower compared to Excel and observed data, indicating that the connection between the friction soil and shallow rock in GMS MODFLOW needs to include fractures, to be able to simulate the responses.

The change in head, seen in table 5.10, are the values obtained from steady-state conditions. However in reality, the soil infiltrations which were only performed during a few days have most likely not reached steady state yet, thus the observed data is not completely representative. Another point, which can affect the modelled change in head during the infiltrations, is the infiltration in Göta älv. As described in section 4.1, the leakage into Göta älv is slightly larger than the infiltrations in the tunnel, see table B.3, and the modelled data could therefore reach higher levels compared to the observed data. However, since the models are simulated as steady-state, this assumption is regarded acceptable.

In this study values of the transmissivity and radius of influence have been calculated and then later used in the models. As seen in appendices C.1.1 and C.1.2 the values vary, indicating that the friction soil varies in thickness and properties. Due to the fluctuating values in transmissivity, the values were decided to be varied depending on the direction in the Excel models. However, this was not possible for all infiltration models and the regional transmissivity or the average of the calculated transmissivities were assigned instead. These values were assumed to account for the differences in the studied area better compared to the local transmissivity, see table 3.1 in chapter 3.

6.3 Suggested infiltration at Residenset

This study focused partly on Residenset, and the aim was to investigate what type of infiltration would be the most suitable for the risk object. Soil infiltration has often been used to raise the groundwater level around buildings, that have a foundation which is prone to settlements (Olofsson & Palmgren, 1994). This could be an option for Residenset, and the modelling performed in this study have showed that soil infiltration can increase the groundwater level close to the infiltration well. However, since the area around Residenset is very densely built, there might be issues with fitting an infiltration facility close by the risk object. Since the soil infiltrations from the modelling showed a more exponential response, the well would have to be built close by the building which in this case might not be possible. Additionally, the exponential curve from the soil infiltration, makes it more difficult to predict the increase in groundwater level since it very rapidly decreases in response. Furthermore, as described in section 2.2, a soil infiltration is prone to clogging if the infiltration flow is too low. Thus, if a soil infiltration was constructed at Residenset and the desired response required only a minor flow, the risk of clogging would increase significantly.

When looking at rock infiltration as an alternative for Residenset, Västlänkstunneln will be constructed beneath the building and Göta älv is located to the east. This

enables implementing rock infiltration in the underground constructions which can potentially reach the overlying aquifer in the friction soil through the fractures. The models in Excel and MODFLOW show a more linear response in rock compared to soil. A benefit from this could be that it is easier to get a response from the rock infiltration, even if the infiltration facility is located further away. On the other hand, a disadvantage might be that the groundwater table will be raised on unwanted locations.

Taking these views into consideration, infiltration in the underlying rock tunnel may be the best option. Looking at figure 3.4, it shows the location of the planned Västlänkstunneln in relation to the risk object, which lies to the east of the tunnel. As mentioned in chapter 3 the general direction of fractures lies in E-W, enabling water to be transported in the direction of Residenset. Further, the linear response might make it easier to adjust and predict the change in groundwater level to stay within the given action levels, see table 3.2. Since the upper and lower aquifer might be connected at some locations in the area, a too high pressure in the lower aquifer can result in raised water levels in the upper aquifer as well, as mentioned in section 3.2. According to figures 5.4 and 5.9 soil infiltration has a greater risk of causing these type of problems, which may result in leakage into basements. Furthermore, for soil infiltration the limiting space in the area restricts the implementation of a new facility. Additionally, the previous soil infiltration in the adjacent Lilla torget showed poor responses in the surrounding groundwater wells, which suggests that similar results might be expected at Residenset. A possible explanation is that the friction soil layer at Lilla torget is less coherent or very thin. However, as stated previously, when constructing a rock infiltration there might be difficulties connecting the borehole to a fracture set and getting the desired capacity from it. If this is the case a soil infiltration could be implemented as a temporary measure if settlements can be detected at the risk object, since it has shown to be easier to implement quicker, see section 2.2.

7
Conclusion

Constructions underground in urban areas can greatly affect the surrounding buildings due to a decrease of pressure in the aquifer during construction. Consequently, this can lead to drawdown of the water table and ultimately subsidence of adjacent buildings in the area. Artificial infiltration can be used as a mean to infiltrate water directly into the aquifer and thereby maintaining or raising the water table. Västlänken, a railway tunnel currently being built in central Gothenburg, is an example of a construction where this method will be used. This report aimed to investigate the differences when infiltrating water in soil and rock and to answer the question of what type of infiltration can be implemented at Residenset, a building with sensitive foundation located close to the planned Västlänkstunneln. Two different numerical tools, Excel and GMS MODFLOW, were used to model the responses from previously performed soil and rock infiltrations in the area. The main findings are listed below.

1. Both Excel and GMS MODFLOW generally showed linear response when infiltrating in rock and exponential response when infiltrating in soil. These findings correspond with observed data. On the other hand, GMS MODFLOW did not correlate well with Excel and the observed data when it comes to the propagation of the responses according to the calculated Spearman correlation coefficient. Both Excel and the observed data displayed that rock infiltrations propagate further away from the infiltration point, resulting in a more diffusive response, compared to soil infiltration.
2. Both numerical models can be used to simulate the response from soil and rock infiltrations. The GMS MODFLOW model is more complex, with several layers and the option to vary hydraulic and hydrogeological parameters over the area. Consequently this results in a time-consuming, complex model. Excel on the other hand, lacks many of GMS MODFLOW's more complex characteristics but is more intuitive and easy to use. The results from the two models indicated that the Excel model corresponded better with the observed data compared to the GMS MODFLOW model.

3. For the risk object within the block Residenset, rock infiltration might be a more appropriate option compared to soil infiltration. This is a result of the infiltration in rock showing a more linear response with a larger propagation, and since the tunnel will be built close by, this gives the right preconditions for rock infiltration. Further, implementing a soil infiltration close to the risk object might be difficult due to the densely built area. Since the soil infiltration has showed a more exponential response it would have to be built close by to raise the groundwater levels sufficiently.

However, what has been observed during this study, is that the infiltrations in both rock and soil are very dependent on the local site characteristics. Connectivity of fractures, thickness and extent of the friction soil and lower aquifer, hydrogeological parameters, are a few examples of factors impacting the results of any infiltration facility. Consequently, these variables have to be characterised and conceptualized in order to perform a successful infiltration. This also results in that the findings in this study might be depending on the local site characteristics, and a similar study performed elsewhere might show other results.

As a future recommendation, primarily it would be interesting to see a similar comparison between soil and rock infiltrations, at another location, to see how site specific the results in this report are. Also, this thesis have not focused on environmental aspects or economic costs connected to artificial infiltration, such as using recycled tunnel water. Consequently, this is something that could be investigated further and can potentially give another perspective to the comparison between soil and rock infiltrations.

Bibliography

Ahmed, N., Sheng, Z., & Taylor, S. (2014). *Hydraulics of wells : Design, construction, testing, and maintenance of water well systems.* American Society of Civil Engineers. https://doi.org/10.1061/9780784412732

Anderson, M., Woessner, W., & Hunt, R. (2015). *Applied groundwater modeling - simulation of flow and advective transport.* (2nd edition). Elsevier. https://doi.org/10.1111/gwat.12464

Ankor, M. J., & Tyler, J. J. (2019). Development of a spreadsheet-based model for transient groundwater modelling. *Hydrogeology Journal*, *27*(5), 1865–1878. https://doi.org/10.1007/s10040-019-01996-z

Aquaveo. (2011). *Gms 8.2 tutorial, modflow – nwt, use modflow-nwt with a simple model.* Aquaveo. Retrieved 2021-05-07, from: http://gmstutorials-8.2.aquaveo.com/MODFLOW-NWT.pdf

Aquaveo. (2017). *Gms:tin module.* XMSWIKI. Retrieved 2021-05-05, from: https://www.xmswiki.com/wiki/GMS:TIN_Module

Aquaveo. (2018). *Gms:wel package.* XMSWIKI. Retrieved 2021-04-29, from: https://www.xmswiki.com/wiki/GMS:WEL_Package

Aquaveo. (2019). *Gms:conductance.* XMSWIKI. Retrieved 2021-04-23, from: https://www.xmswiki.com/wiki/GMS:Conductance

Aquaveo. (n.d-a). *Gms - groundwater modeling system.* Aquaveo. Retrieved 2021-05-05, from: https://www.aquaveo.com/software/gms-groundwater-modeling-system-introduction

Aquaveo. (n.d-b). *Modflow modeling in gms.* Aquaveo. Retrieved 2021-05-05, from: https://www.aquaveo.com/software/gms-modflow

Axelsson, C.-L., & Follin, S. (2000). *Grundvattensänkning och dess effekter vid byggnation och drift av ett djupförvar* (r-00-21). Svensk Kärnbränslehantering AB. https://skb.se/upload/publications/pdf/R-00-21.pdf

Cashman, P., Preene, M., & Rosser, M. (2020). *Groundwater lowering in construction - a practical guide to dewatering* (3rd edition). Taylor & Francis Group. https://doi.org/10.1201/9781003050025

Eniro. (2021). [GÖTEBORG, INOM VALLGRAVEN] Retrieved: 2021-05-21, from: https://kartor.eniro.se/?c=57.705543,11.962245&z=17

Fetter, C. W. (2014). *Applied hydrogeology* (4th edition). Pearson Education Limited.

Gustafson, G. (2009). *Hydrogeologi för bergbyggare.* Formas.

Gustafson, G., & Svensson, C. (1994). *GROUNDWATER MODELLING USING A SPREAD-SHEET COMPUTER PROGRAM* (CTH - Publication No. C 50, version 1.9).

Haan, C. T., Barfield, B. J., & Hayes, J. C. (1994). *Design hydrology and sedimentology for small catchments* (3rd edition). (pp. 435-436). Elsevier. https://doi.org/10.1016/B978-0-08-057164-5.50016-5

Hölting, B., & Coldewey, W. G. (2019). *Hydrogeology*. Springer Berlin Heidelberg. doi:%2010.1007/978-3-662-56375-5

Iversen, G. R., & Gergen, M. (1997). *Statistics, the conceptual approach*. Springer, New York, NY. https://doi.org/10.1007/978-1-4612-2244-6_12

Kvartsberg, S., Thörn, J., Runslätt, E., & Almfeldt, S. (2021). *BERÄKNINGSMETOD FÖR INJEKTERINGSDESIGN - UTREDNING AV MODELLANTAGANDE*. [BEFO NO. 177]. Stiftelsen Bergteknisk forskning.

Lindström, M., & Kveen, A. (2005). *Tunnel investigation and groundwater control* (no. 107). Statens Vegvesen. http://hdl.handle.net/11250/191622

Ojha, C. S. P., Singh, V. P., & Adrian, D. D. (2003). Determination of critical head in soil piping. *Journal of Hydraulic Engineering*, *129*(7), 511–518. https://doi.org/10.1061/(ASCE)0733-9429(2003)129:7(511)

Olofsson, B., & Palmgren, S. (1994). *Djupinfiltration för grundvattennivåkontroll* (no. 13). Stiftelsen Svensk Bergteknisk Forskning. https://www.befoonline.org/UserFiles/Archive/90/Sve-BeFo-Rapport13.pdf

Phien-wej, N., Giao, P., & Nutalaya, P. (1998). Field experiment of artificial recharge through a well with reference to land subsidence control. *Engineering Geology*, *50*(1), 187–201. https://doi.org/10.1016/S0013-7952(98)00016-7

Rafi, J. Y. (2014). *Study of pumping pressure and stop criteria in grouting of rock fractures* [(Doctoral dissertation). KTH Royal Institute of Technology]. Source: DiVA. https://www.diva-portal.org/smash/get/diva2:760821/FULLTEXT01.pdf.

SMHI. (n.d). *Ladda ner meteorologiska observationer*. Retrieved 2021-03-20, from: https://www.smhi.se/data/meteorologi/ladda-ner-meteorologiska-observationer/

Trafikverket. (2016a). *Ingenjörsgeologisk prognos* (Västlänken - Publication No. E00-17-025-0000-0100).

Trafikverket. (2016b). *PM Hydrogeologi berg - Underlagsdokument till PM Hydrogeologi, ansökan om tillstånd vattenverksamhet* (Västlänken och Olskroken planskildhet - Publication No. MPU02-50GT-025-00-0004). https://m.trafikverket.se/contentassets/c19fd7547e2b493688f3cc0576742d31/26_4_pm_hydrogeologi_berg.pdf

Trafikverket. (2016c). *PM Hydrogeologi jord - Underlagsdokument till PM Hydrogeologi, ansökan om tillstånd enligt miljöbalken för anläggandet av Västlänkan och Olskrokens planskildhet* (Publication No. MPU02-50GT-025-00-0005). https://www.trafikverket.se/contentassets/c19fd7547e2b493688f3cc0576742d31/26_5_pm_hydrogeologi_jord.pdf

Trafikverket. (2016d). *Tekniskt PM Bergteknik Bilaga 3, Otterhällan* (Västlänken - Publication No. E04-17-025-0500-0005).

Trafikverket. (2017a). *Tillståndsansökan för vattenverksamhet - Kvartersbeskrivning Inom Vallgraven 52*. (Västlänken och Olskroken planskildhet - Publication No. MPU02-01-036-IV52-0001).

Trafikverket. (2017b). *Tillståndsansökan för vattenverksamhet - Kvartersbeskrivning Inom Vallgraven 53*. (Västlänken och Olskroken planskildhet - Publication No. MPU02-01-036-IV53-0001).

Trafikverket. (2017c). *Tillståndsansökan för vattenverksamhet - Kvartersbeskrivning Inom Vallgraven 55.* (Västlänken och Olskroken planskildhet - Publication No. MPU02-01-036-IV55-0001).

Trafikverket. (2017d). *Tillståndsansökan för vattenverksamhet - Kvartersbeskrivning Inom Vallgraven 59.* (Västlänken och Olskroken planskildhet - Publication No. MPU02-01-036-IV59-0001).

Trafikverket. (2017e). *Tillståndsansökan för vattenverksamhet - Kvartersbeskrivning Nordstaden 21.* (Västlänken och Olskroken planskildhet - Publication No. MPU02-01-036-NS21-0001).

Trafikverket. (2017f). *Tillståndsansökan för vattenverksamhet - Kvartersbeskrivning Nordstaden 27.* (Västlänken och Olskroken planskildhet - Publication No. MPU02-01-036-NS27-0001).

Trafikverket. (2017g). *Tillståndsansökan för vattenverksamhet - Kvartersbeskrivning Nordstaden 36.* (Västlänken och Olskroken planskildhet - Publication No. MPU02-01-036-NS36-0001).

Trafikverket. (2017h). *Tillståndsansökan för vattenverksamhet - Kvartersbeskrivning Nordstaden 37.* (Västlänken och Olskroken planskildhet - Publication No. MPU02-01-036-NS37-0001).

Trafikverket. (2019). *Skydd av grundvatten inom projekt västlänken.* Retrieved 2021-03-09, from: https://www.trafikverket.se/nara-dig/Vastra-gotaland/vi-bygger-och-forbattrar/Vastlanken---smidigare-pendling-och-effektivare-trafik/Vastlankens-miljoarbete/skydd-av-grundvatten/

Trafikverket. (2020). *PM Låga grundvattennivåer Inom Vallgraven och Nordstaden hösten 2018* (Västlänken och Olskroken planskildhet - Publication No. BUT01-50GT-025-0000-0_0 − 0021)..

Vägverket. (2000). *Tätning av bergtunnlar – förutsättningar, bedömningsgrunder och strategi vid planering och utformning av tätningsinsatser* (no.101). https://trafikverket.ineko.se/Files/sv-SE/10421/RelatedFiles/2000_101_tatning_av_bergtunnlar.pdf

Vestin, T., Nilsson, A., Höög, K., Larsson, J., Lindström, M., Ljung, S., Torle, J., & Munkenberg, B.-A. (2016). *Västlänken och olskroken planskildhet - göteborg stad och mölndals stad, västra götalands län - kontrollprogram grundvatten* (trv 2016/3151). Trafikverket. https://www.trafikverket.se/contentassets/623cad16101d40edbc580de82cd93ee6/kontrollprogram_grundvatten.pdf

Yoo, C. (2016). Ground settlement during tunneling in groundwater drawdown environment – influencing factors. *Underground Space*, *1*(1), 20–29. https://doi.org/10.1016/j.undsp.2016.07.002

Zhang, Y.-Q., Wang, J.-H., Chen, J.-J., & Li, M.-G. (2017). Numerical study on the responses of groundwater and strata to pumping and recharge in a deep confined aquifer. *Journal of Hydrology*, *548*, 342–352. https://doi.org/10.1016/j.jhydrol.2019.03.079

Zheng, G., Ha, D., Zeng, C., Cheng, X., Zhou, H., & Cao, J. (2019). Influence of the opening timing of recharge wells on settlement caused by dewatering in excavations. *Journal of Hydrology*, *573*, 534–545. https://doi.org/10.1016/j.jhydrol.2019.03.079

A

Appendix 1

A.1 Observed data from the infiltration sites

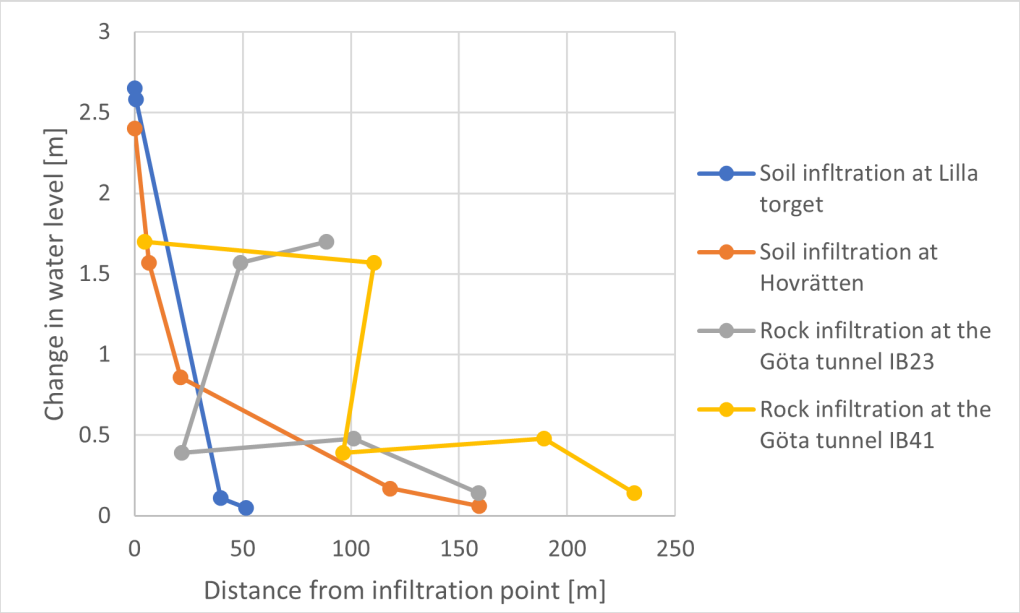

Figure A.1: Plot of observed data from rock and soil infiltrations

B

Appendix

B.1 Götatunneln leakage vs. infiltration 2013 - 2017

In tables B.1 and B.2, data about leakage and infiltration rates for Götatunneln can be seen. Regarding the leakage measurements, all the measurements south of the Stora Hamnkanalen, within the study area were selected. By comparing the total leakage and the total infiltration, it was determined that the leakage rate into the tunnel is approximately 1.73 l/min higher than the infiltration rate over the studied stretch. Additionally, leakage measurements not related to Götatunneln were omitted.

	GT B 20/280	GT B4Södra 2/000	GT B4 Norra 21/095	GT B4Södra 2/110
2013	NA	2.61	1.58	1.76
2014	1.20	3.00	1.55	1.70
2015	1.70	2.03	1.35	1.72
2016	1.20	2.03	1.53	1.45
2017	1.20	2.40	1.50	1.85
Ave	**1.33**	**2.42**	**1.50**	**1.68**
Std	0.22	0.39	0.08	0.14

Table B.1: The leakage rate [l/min] into Götatunneln between 2013 and 2017.

	IB23	IB41	IB55	IB61	IB64
2013	2.40	1.65	0.19	0.47	0.40
2014	2.53	1.79	0.18	0.44	0.39
2015	2.52	1.71	0.21	0.50	0.24
2016	2.79	1.72	0.20	0.50	0.25
2017	2.59	1.49	0.15	0.40	0.26
Ave	**2.56**	**1.67**	**0.18**	**0.46**	**0.31**
Std	0.13	0.10	0.02	0.04	0.07

Table B.2: The infiltration rate [l/min] in Götatunneln IB23, IB41, IB55, IB61, IB64 between 2013 and 2017.

	Total rate [l/min]
Leakage	6.92
Infiltration	5.19

Table B.3: The total leakage and infiltration rate [l/min] between 2013 and 2017, based on the average values in tables B.1 and B.2.

C
Appendix

C.1 Analytical caluculations

This Appendix shows the calculated values of the transmissivity and radius of influence.

C.1.1 Transmissivity

All the transmissivities for the different scenarios can be found in this section. Numbers marked in bold text were either applied in the model or used to calculate an average hydraulic conductivity described in section 4.4.1.

	CH4218U	GW1916A	GWI101
T_T [m^2/s]	**3.68E-04**	**3.47E-05**	**3.41E-05**
$T_{C.J}$ [m^2/s]	1.89E-05	1.33E-04	6.23E-05

Table C.1: Calculated transmissivity values [m^2/s] using the Cooper-Jacob, $T_{C.J}$, and the Thiem's equations, T_T, for Lilla torget.

	CH4267U	GW1914	CH4218U	CH4336U
T_T [m^2/s]	4.10E-05	4.84E-05	**4.03E-05**	7.66E-05
$T_{C.J}$ [m^2/s]	**4.92E-06**	**1.87E-05**	1.50E-04	**5.61E-05**

Table C.2: Calculated transmissivity values [m^2/s] using the Cooper-Jacob, $T_{C.J}$, and the Thiem's equations, T_T, for Hovrätten.

	GW1918	GWI113	GW1914	GW1915A
T_T [m^2/s]	**6.44E-06**	**4.14E-06**	4.77E-05	**1.02E-04**

Table C.3: Calculated transmissivity values [m^2/s] using Thiem's equation, T_T, for Göta tunnel IB23.

	CH4286B	GWI113	GW1914	GW1915A
T_T [m^2/s]	**7.50E-06**	**7.90E-05**	**7.70E-05**	**9.84E-06**

Table C.4: Calculated transmissivity values [m^2/s] using Thiem's equation, T_T, for Göta tunnel IB41.

C.1.2 Radius of influence

In this section the calculated radius of influence can be found. The table for each infiltration shows the radius calculated by equation 4.3 and the figure shows a scatter plot of all observed data used in the model, linear regression analysis and a weighted curve in accordance with the conditions of the observations wells. Notice, some tables includes N/A, which is used when the value was interpreted to be uncertain.

Table C.5 shows the results generated by equation 4.3 at Lilla torget.

	CH4286B	CH4218U	GW1916A	GWI101
Distance	Ref.Well	N/A	57.98 [m]	51.71 [m]

Table C.5: Calculated radius of influence for Lilla torget [m].

Figure C.1 shows the results generated from the plotted values and the regression analysis. The points in the graph corresponds to the values obtained in the observation wells and the curves describes the obtained result from the regression analysis and the weighting of the curve due to the condition of the wells. The R-square value for the regression analysis was 0.96.

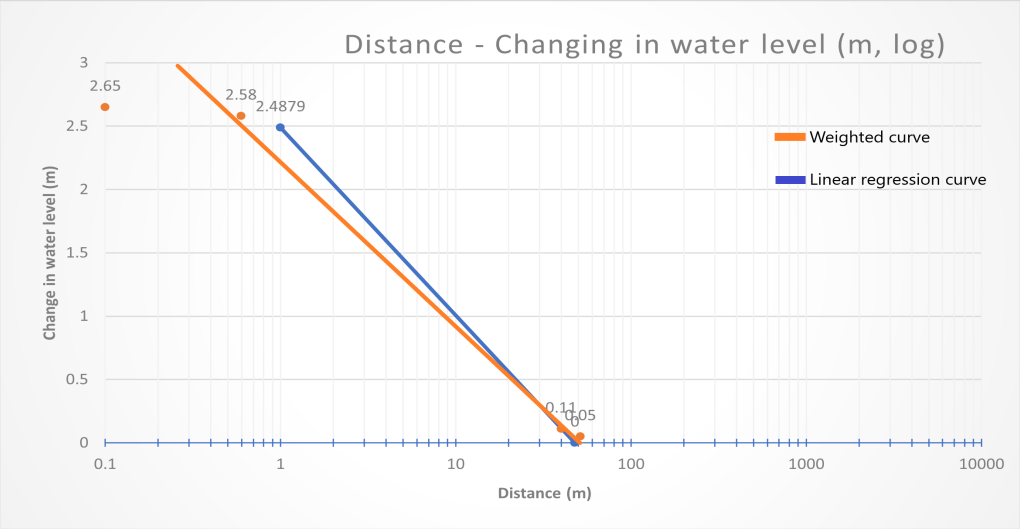

Figure C.1: Radius of influence generated by regression at Lilla torget and the weight curve.

Table C.6 shows the results generated by equation 4.3 at Hovrätten.

	CH4337B	CH4267U	CH4336U	GW1914	CH4218U
Distance	Ref.Well	0.27 [m]	N/A	0.54 [m]	0.25 [m]

Table C.6: Calculated radius of influence for Hovrätten [m].

Figure C.2 shows the result generated from the plotted values and the regression analysis. The points in the graph corresponds to the values obtained in the observation wells and the curves describe the obtained results from the regression analysis and the weighting of the curve due to the conditions of the wells. The R-square value for the regression analysis was 0.82.

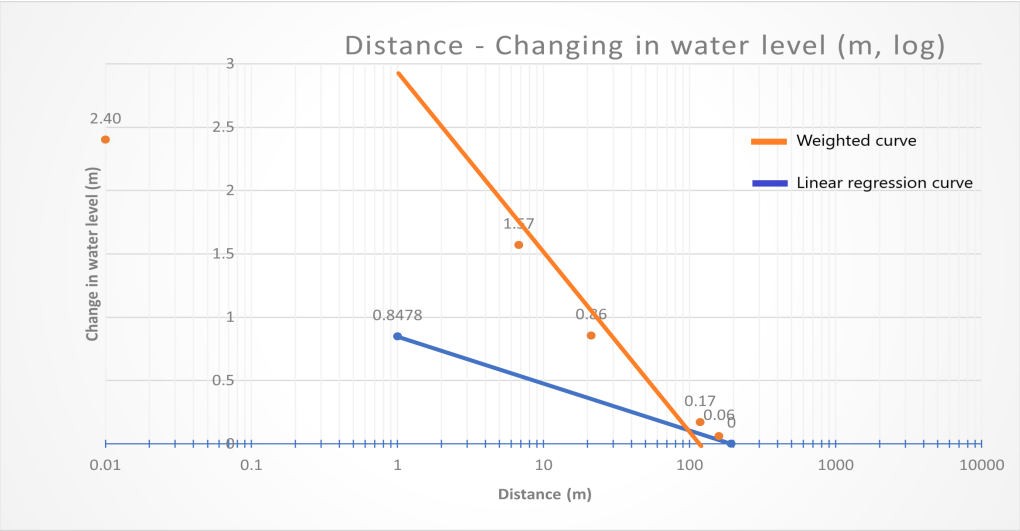

Figure C.2: Radius of influence generated by regression at Hovrätten and the weighted curve.

Table C.7 and C.8 displays the calculated radius of influences for Göta tunnel IB23 and IB41.

	CH4286B	GWI113	GW1918	GW1915A	GW1914
Distance	Ref.Well	28.39 [m]	32.98 [m]	N/A	485.77[m]

Table C.7: Calculated radius of influence for Göta tunnel IB23 [m].

	GW1918	GWI113	CH4286B	GW1915A	GW1914
Distance	Ref.Well	N/A	237.58 [m]	814.71 [m]	264.15[m]

Table C.8: Calculated radius of influence for Göta tunnel IB41 [m].

Figure C.3 shows the results generated from the plotted values. Since the observed data is scattered and the boreholes used the same observation wells, the regression analysis generated a low R-square value, thus no reliable regression curve was obtained. The curves in the graph are weighted in relation to the condition of the observation wells.

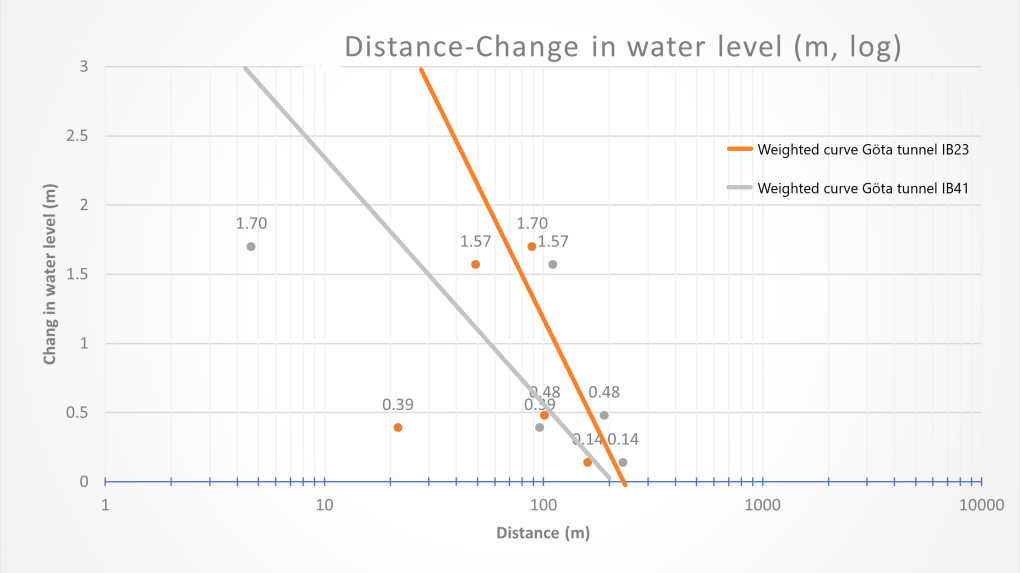

Figure C.3: The levels in the observation wells vs. the distance from the infiltration facilities in the Göta tunnel.

D

Appendix

D.1 Rock calibration model

In figure D.1 and table D.1, the results generated by the rock calibration model in Excel can be seen.

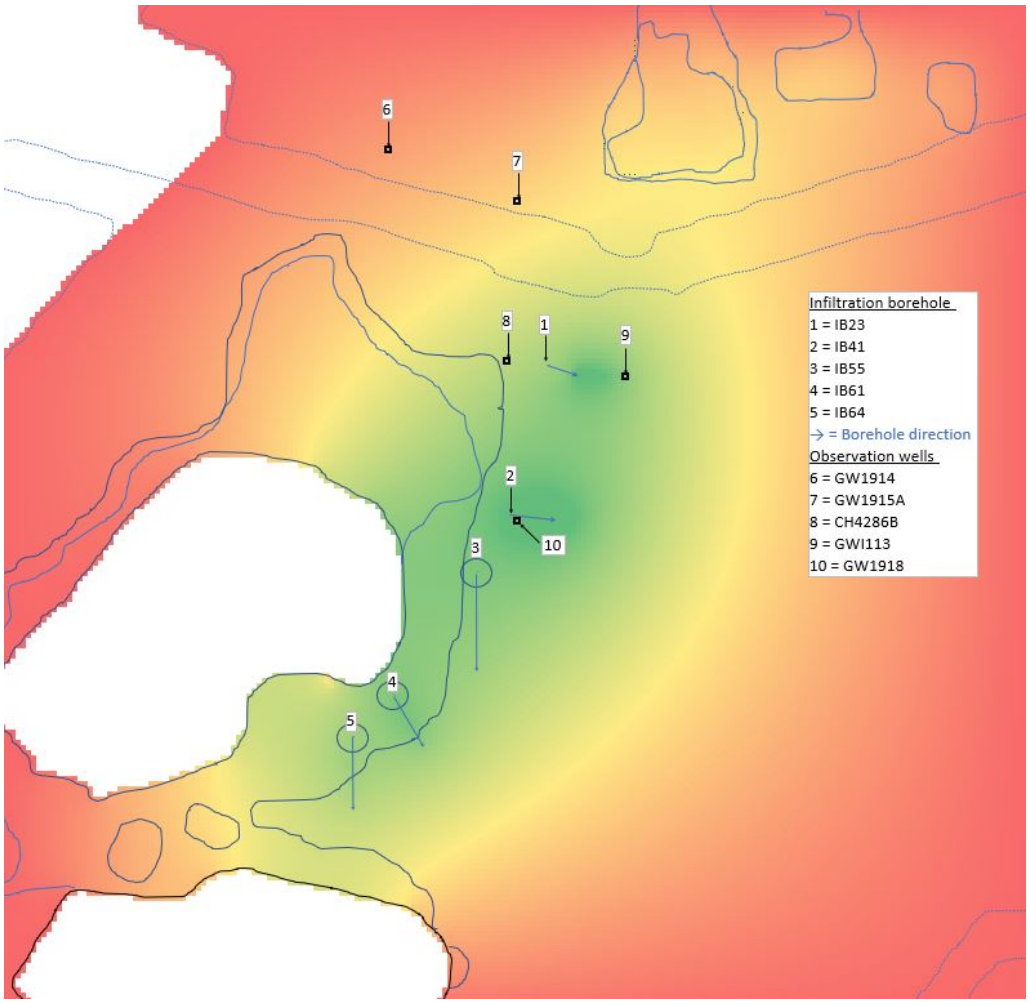

Figure D.1: The propagation generated from the rock calibration model in Excel.

Well	GW1918	GWI113	CH4286B	GW1915A	GW1914
Observed value [m]	1.70	1.570	0.47	0.39	0.14
Model value [m]	1.07	0.80	0.717	0.43	0.21

Table D.1: The change in water level when Göta tunnel IB23, IB41, IB55, IB61, IB64 were applied in the Excel rock calibration model.

DEPARTMENT OF SOME SUBJECT OR TECHNOLOGY
CHALMERS UNIVERSITY OF TECHNOLOGY
Gothenburg, Sweden
www.chalmers.se

CHALMERS
UNIVERSITY OF TECHNOLOGY